

DTIC FILE COPY

4

AD

AD-E401 833

AD-A198 204

TECHNICAL REPORT ARAED-TR-88010-

# A PRELIMINARY FLEXIBLE FIN DEPLOYMENT SIMULATION

WALTER KOENIG

DTIC  
ELECTRIC  
AUG 08 1988  
S H D

AUGUST 1988



US ARMY  
ARMAMENT MUNITIONS  
& CHEMICAL COMMAND  
ARMAMENT RDE CENTER

U. S. ARMY ARMAMENT RESEARCH, DEVELOPMENT AND ENGINEERING CENTER

ARMAMENT ENGINEERING DIRECTORATE

PICATINNY ARSENAL, NEW JERSEY

APPROVED FOR PUBLIC RELEASE: DISTRIBUTION IS UNLIMITED.

88 8 08 116

The views, opinions, and/or findings contained in this report are those of the author(s) and should not be construed as an official Department of the Army position, policy, or decision, unless so designated by other documentation.

The citation in this report of the names of commercial firms or commercially available products or services does not constitute official endorsement by or approval of the U.S. Government.

Destroy this report when no longer needed by any method that will prevent disclosure of contents or reconstruction of the document. Do not return to the originator.

# REPORT DOCUMENTATION PAGE

1a. REPORT SECURITY CLASSIFICATION <b>UNCLASSIFIED</b>			1b. RESTRICTIVE MARKINGS		
2a. SECURITY CLASSIFICATION AUTHORITY			3. DISTRIBUTION/AVAILABILITY OF REPORT		
2b. DECLASSIFICATION/DOWNGRADING SCHEDULE			Approved for public release; distribution is unlimited.		
4. PERFORMING ORGANIZATION REPORT NUMBER Technical Report ARAED-TR-88010			5. MONITORING ORGANIZATION REPORT NUMBER		
6a. NAME OF PERFORMING ORGANIZATION ARDEC, AED		6b. OFFICE SYMBOL SMCAR-AET-A	7a. NAME OF MONITORING ORGANIZATION		
6c. ADDRESS (CITY, STATE, AND ZIP CODE) Armament Technology Div Picatinny Arsenal, NJ 07806-5000			7b. ADDRESS (CITY, STATE, AND ZIP CODE)		
8a. NAME OF FUNDING/SPONSORING ORGANIZATION STINFO Br		8b. OFFICE SYMBOL SMCAR-IMI-I	9. PROCUREMENT INSTRUMENT IDENTIFICATION NUMBER		
8c. ADDRESS (CITY, STATE, AND ZIP CODE) Picatinny Arsenal, NJ 07806-5000			10. SOURCE OF FUNDING NUMBERS		
			PROGRAM ELEMENT NO.	PROJECT NO.	TASK NO. WORK UNIT ACCESSION NO.
11. TITLE (INCLUDE SECURITY CLASSIFICATION)  A PRELIMINARY FLEXIBLE FIN DEPLOYMENT SIMULATION					
12. PERSONAL AUTHOR(S) Walter Koenig					
13a. TYPE OF REPORT Final		13b. TIME COVERED FROM May 84 to Aug 87		14. DATE OF REPORT (YEAR, MONTH, DAY) August 1988	
15. PAGE COUNT 50					
16. SUPPLEMENTARY NOTATION					
17. COSATI CODES			18. SUBJECT TERMS (CONTINUE ON REVERSE IF NECESSARY AND IDENTIFY BY BLOCK NUMBER)		
FIELD	GROUP	SUB-GROUP			
			Flexible fin Samara Auto gyro		
			Maple seed Decelerator Deployment simulation		
19. ABSTRACT (CONTINUE ON REVERSE IF NECESSARY AND IDENTIFY BY BLOCK NUMBER)					
<p>A simulation for modeling the deployment of a flexible-fin decelerator from a spinning body is described. This decelerator is typically used to drive a submunition in a lunar motion while it descends over a battlefield scanning for armored targets. This decelerator consists of a single flexible fin with a weighted tip and was developed at the U.S. Army Research, Development and Engineering Center.</p> <p>The decelerator is modeled as a series of masses connected by flexible elements. The motion of the masses is determined only by tension forces since aerodynamic forces are not considered in this effort. Two dimensional equations of motion for each mass are solved by a fourth order Runge-Kutta routine.</p> <p>Test cases were run for three different fin packing techniques: lumping all of the fin masses and tip weight at the root, positioning the fin around the periphery of the submunition wrapped in the spin direction, and position the</p> <p style="text-align: right;">(cont)</p>					
20. DISTRIBUTION/AVAILABILITY OF ABSTRACT			21. ABSTRACT SECURITY CLASSIFICATION		
<input type="checkbox"/> UNCLASSIFIED/UNLIMITED <input checked="" type="checkbox"/> SAME AS RPT. <input type="checkbox"/> DTIC USERS			UNCLASSIFIED		
22a. NAME OF RESPONSIBLE INDIVIDUAL I. HAZNEDARI			22b. TELEPHONE (INCLUDE AREA CODE) (201)724-3316		22c. OFFICE SYMBOL SMCAR-IMI-I

19. ABSTRACT: (cont)

fin around the periphery wrapped opposite the spin direction. The best packing method was found to be wrapping the fin around the submunition in the spin direction. This resulted in the cleanest deployment and lowest tension loads (750 lb).

The other two simulated methods resulted in tension loads in excess of 800 lb, the assumed breaking strength of the fin.

Accession For	
NTIS GRA&I	<input checked="checked" type="checkbox"/>
DTIC TAB	<input type="checkbox"/>
Unannounced	<input type="checkbox"/>
Justification	
By	
Distribution/	
Availability Codes	
Dist	Avail and/or Special
A-1	

## CONTENTS

	Page
Introduction	1
Discussion	1
Results	2
Conclusions	4
References	33
Glossary	35
Appendix - Closed Form Solution of Simple Two Body Problem	37
Distribution List	43

## FIGURES

1	Smart submunition operational sequence	7
2	Submunition/flexible fin system	8
3	System model	9
4	Simulation coordinate system	10
5	Simulation flowchart	11
6	Simulated packing techniques	12
7	Deployment sequence, sequential deployment from root	13
8	Tensions versus time for sequential deployment from root	14
9	Deployment sequence, fin wrapped in spin direction	19
10	Tensions versus time for fin wrapped in spin direction	21
11	Deployment sequence, fin wrapped opposite to spin direction	26
12	Tensions versus time for fin wrapped opposite to spin direction	28

## INTRODUCTION

A flexible-fin decelerator to orient and stabilize "smart" submunitions has been developed and patented (ref 1). These submunitions are ejected from a rapidly spinning projectile and descend vertically over a battlefield, searching for armored targets (fig. 1). The flexible fin drives the submunition in a lunar motion at a predetermined steady state spin rate and fall velocity. A lunar motion is required for target scan and for the sensor to lead the warhead axis.

Since the submunitions are ejected from a rapidly spinning projectile (up to 260 Hz), reliable deployment of the flexible fin could be a problem.

The objective of the present work is to develop a numerical simulation to model the deployment of a flexible-fin decelerator from a rapidly spinning body. Such a simulation allows for the evaluation of various fin packing techniques and fin strength without resorting to the usual cut-and-try test procedures. (JFS) ←

The method uses an approach similar to that of Purvis (refs 2 and 3) in which the decelerator is modeled as a series of masses connected by flexible elements. The motion of the masses is determined solely by tension forces; aerodynamic forces will be included in future efforts. Further limitations to this study are constant submunition spin rate and two-dimensional motion confined to the plane of the top of the submunition.

## DISCUSSION

The system to be simulated consists of the submunition body, the flexible fin, and the tip weight (fig. 2). The fin is modeled as a series of masses connected to each other (and to the body and tip weight) by springs and dampers. A drawing of the system model with the fin stretched out is shown in figure 3. The undeflected length of the fin elements is  $s_{0i}$ .

The equations of motion of a given mass are:

$$m\ddot{x}_i = (T_i + D_i)\cos\theta_i - (T_{i-1} + D_{i-1})\cos\theta_{i-1} \quad (1)$$

$$m\ddot{y}_i = (T_i + D_i)\sin\theta_i - (T_{i-1} + D_{i-1})\sin\theta_{i-1} \quad (2)$$

The coordinate system and angular definitions are shown in figure 4. The only forces assumed to act on the masses are tension and damping forces. Tension and damping between masses  $i$  and  $i-1$  are  $T_i$  and  $D_i$ , respectively. Tension is computed by calculating the distance between the masses ( $s_i$ ) and comparing it to the undeflected distance ( $s_{0i}$ ). If  $s_i$  is less than  $s_{0i}$ , tension is zero. The spring constant is calculated using the breaking strength and percent elongation at breaking of the fin material:

$$k = \frac{F_{Br}}{\epsilon_{Br} s_{0i}} \quad (3)$$

Tension is given by:

$$T_i = (s_i - s_{o_i})k \quad (4)$$

Damping is assumed linearly proportional to the velocity of one mass relative to the other. The distance between masses is given by:

$$s_i = \sqrt{(x_i - x_{i-1})^2 + (y_i - y_{i-1})^2} \quad (5)$$

The derivative of this quantity is the relative velocity:

$$\dot{s}_i = \frac{[(x_i - x_{i-1})(\dot{x}_i - \dot{x}_{i-1}) + (y_i - y_{i-1})(\dot{y}_i - \dot{y}_{i-1})]}{\sqrt{(x_i - x_{i-1})^2 + (y_i - y_{i-1})^2}} \quad (6)$$

Therefore, damping is given by:

$$D_i = C_d \dot{s}_i \quad (7)$$

where  $C_d$  is the damping coefficient. As with the tension, if  $s_i$  is less than  $s_{o_i}$ , damping is zero.

A flow chart of the deployment simulation is shown in figure 5. A fourth order Runge-Kutta routine is used to solve the equations of motion for each mass.

## RESULTS

Several test cases were run to demonstrate the simulation and evaluate three different fin packing techniques. The submunition weight was 10 lb and had a diameter of 5 in. The spin rate chosen was 450 rad/s, representative of the spin rate at cargo ejection of a low zone 155-mm firing. The fin had a 10-in. span, 3-in. chord, weighed 0.02 lb, and was divided into 4 masses (0.005 lb each). The tip mass weighed 0.2 lb. For these preliminary cases, the damping coefficient ( $C_d$ ) was set to zero. The fin breaking strength was assumed to be 800 lb and elongation at breaking ( $\epsilon_{Br}$ ) 25%.

When dealing with relatively small masses and large spring constants, system frequencies can be high. Choosing a small enough timestep is crucial if large errors are to be avoided. The smallest mass and largest spring constant can be used to calculate the highest frequency possible in the system. This frequency is given by:

$$W_{\max} = \sqrt{\frac{k_{\max}}{m_{\min}}} \quad (8)$$

The maximum spring constant is obtained from equation 3 using the undeflected length between fin masses ( $s_0$ ), in this case 2.0 inches. From equation 3,  $k_{\max} = 19,200$  lb/ft. The smallest mass in the system is a fin mass, 0.005 lb. From equation 8,  $\omega_{\max} = 11,120$  rad/s. The period is 0.00056 sec.

To test the effect of the size of the timestep, the simple case of two fin masses connected with a 2.0-in. long spring was simulated. At time zero, one of the masses is given an initial velocity of 94 ft/s. The position and velocity versus time of this mass can then be compared to the analytic solution. The exact solution is compared to the simulation for the indicated time step in table 1. Since the velocity varies sinusoidally about 47.0 ft/s, the difference in velocity is normalized with the average velocity, 47.0 ft/s. The difference in position is normalized with the exact position. For a timestep of 0.000025 sec, the simulated position and velocity deviates less than 2% from the exact solution. For the test cases described below, a timestep of 0.000025 sec was used, roughly 20 integrations per cycle.

The first simulated packing technique was lumping all of the fin masses and tip weight at the fin root (fig. 6a). The tip weight was given the tangential velocity at the outside edge of the submunition (S/M) and was free to deploy. When the tip mass moved far enough away from the S/M to put tension between it and the first fin mass, the first fin mass was allowed to deploy. The remaining fin masses were allowed to deploy sequentially in the same manner. The position of each mass and the submunition was plotted with a graphics program. A sequence of these plots, each at a later time, is shown in figure 7. The deployment sequence shows the fin falling behind the submunition and starting to cross over the top. In a tactical environment, aerodynamic loads on the fin (not included in the present simulation) as it is deploying may tend to allow it to "catch up" to the submunition. Tension in the flexible members between the masses is shown in figure 8. The maximum tension calculated was about 1250 lb and occurred between the second and third fin masses. For this packing technique, it is likely that the fin would fail at deployment.

The second simulated packing technique was to position the fin, stretched out, around the periphery of the submunition wrapped in the spin direction (fig. 6b). All of the masses were given the tangential velocity at the outside edge of the submunition and were allowed to deploy at time zero. The resulting deployment sequence (fig. 9) shows the fin to deploy "ahead" of the submunition initially and become fully erect at about 0.012 seconds. The fin then falls behind the submunition, but in a tactical environment and once its erect, aerodynamic forces will keep it erect. Tensions are shown in figure 10. Maximum tension is about 750 lb and occurs between fin mass four and five. The fin strength is adequate for this packing technique.

The third simulated packing technique was to position the fin, stretched out, around the periphery of the submunition, wrapped opposite to the spin direction (fig. 6c). All of the masses were given the tangential velocity at the outside edge of the submunition and were allowed to deploy at time zero. The resulting deployment sequence (fig. 11) shows that the fin immediately crosses the top of the submunition, becomes partially erect, and then falls behind. It is likely that the deployment in this manner will result in a twisted fin. Tensions are shown in figure 12. Maximum tension is about 1400 lb and occurs between mass five and the submunition. Besides twisting, it is likely that the fin would fail at deployment.

The packing technique resulting in the cleanest and lowest deployment loads is wrapping the fin around the submunition periphery in the spin direction.

### CONCLUSIONS

A simulation to model the deployment of a flexible fin decelerator has been developed. At present, motion is confined to two dimensions and determined solely by tension forces. An obvious extension to this work is to add aerodynamic forces and to allow motion in three dimensions. Also, the simulation must be validated by test data.

Of the test cases simulated, the most promising deployment resulted when the fin was wrapped around the periphery of the submunition in the same direction as the submunition spin. This resulted in a clean deployment with the lowest fin tension forces.

Table 1. Comparison of simulation to exact solution

t (sec)	$x_{\text{exact}}$ (ft)	$\dot{x}_{\text{exact}}$ (ft/s)	$\Delta t = 0.0001$		$\Delta t = 0.00005$		$\Delta t = 0.000025$	
			$x_{\text{sim}}$	$\dot{x}_{\text{sim}}$	$x_{\text{sim}}$	$\dot{x}_{\text{sim}}$	$x_{\text{sim}}$	$\dot{x}_{\text{sim}}$
			error (%)	error (%)	error (%)	error (%)	error (%)	error (%)
0.0001	0.007689	46.88	0.007463 2.94	47.86 -2.1	0.007680 0.12	47.10 -0.47	0.007688 0.013	46.93 0.11
0.0002	0.009385	0.0006	0.009501 -1.24	6.85 -14.6	0.009413 -0.30	0.28 -0.59	0.009391 -0.06	0.01 -0.02
0.0003	0.11111	47.36	0.011742 -5.68	44.79 5.5	0.011138 -0.24	47.31 0.11	0.011112 -0.009	47.21 0.32
0.0004	0.018831	94.00	0.018627 1.08	81.24 27.1	0.018774 0.30	93.43 1.2	0.018818 0.07	93.98 0.04
0.0005	0.026489	46.40	0.025510 3.70	50.14 -8.0	0.026444 0.17	47.51 -2.4	0.026487 0.008	46.65 -0.53
0.0006	0.028154	0.0056	0.028422 -0.95	17.84 -37.9	0.028238 -0.30	0.85 -1.8	0.028174 -0.07	-0.03 -0.05
0.0007	0.029912	47.84	0.031190 -4.27	43.24 9.8	0.029974 -0.21	46.30 3.2	0.029914 -0.007	47.48 0.77
0.0008	0.037661	93.99	0.037348 0.83	71.79 47.2	0.037549 0.29	92.87 2.3	0.037635 0.09	93.96 0.06
0.0009	0.045288	45.91	0.043752 3.40	51.12 -11.1	0.045208 0.18	47.90 -4.2	0.045286 0.004	46.38 -1.0
0.0010	0.046923	0.015	0.047269 -0.73	25.96 -55.2	0.047063 -0.30	1.41 -3.0	0.046956 -0.07	0.05 -0.07
0.0011	0.048712	48.33	0.050468 -3.60	42.71 12.0	0.048810 -0.20	45.91 5.1	0.048715 -0.006	47.76 1.2
0.0012	0.056492	93.98	0.056125 0.65	64.83 62.0	0.056324 0.30	92.30 3.6	0.056453 0.07	93.94 0.09

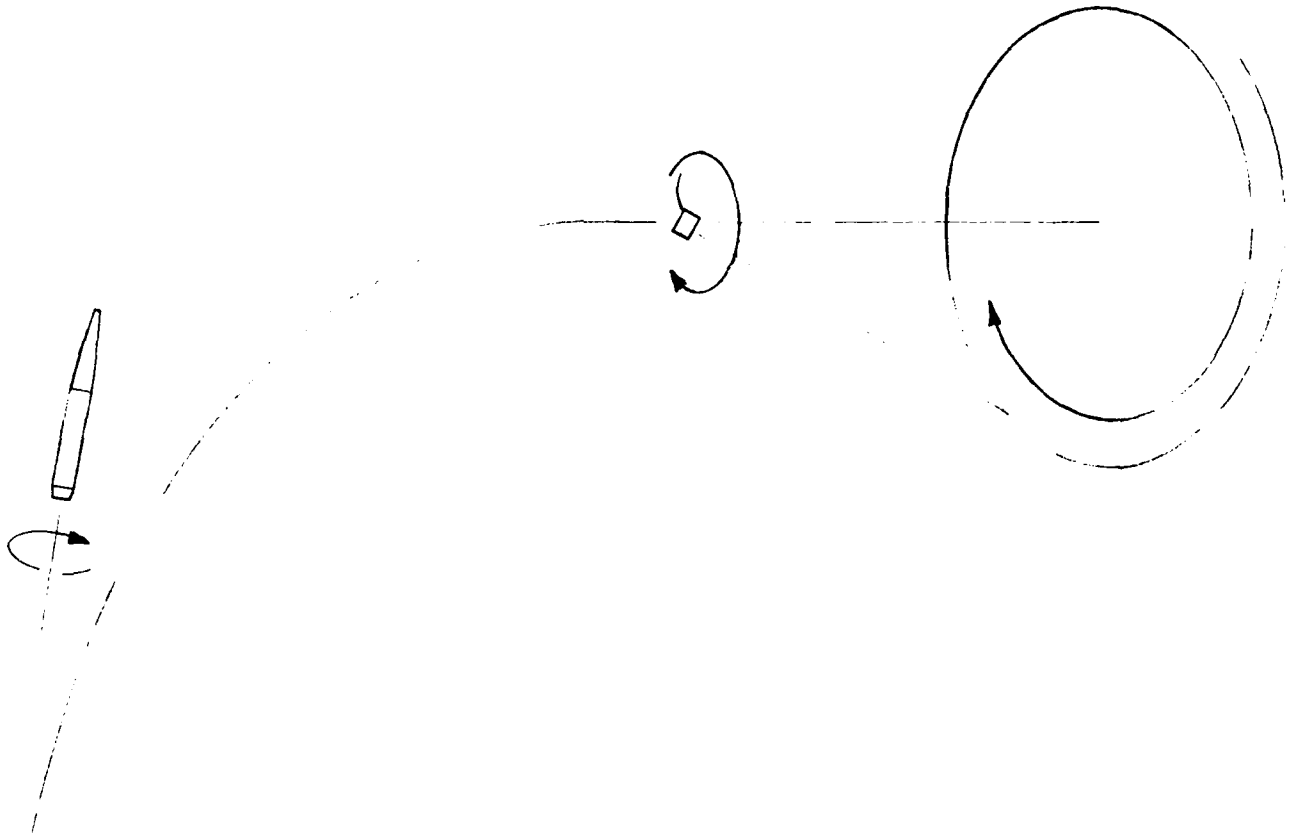


Figure 1. Smart submunition operational sequence

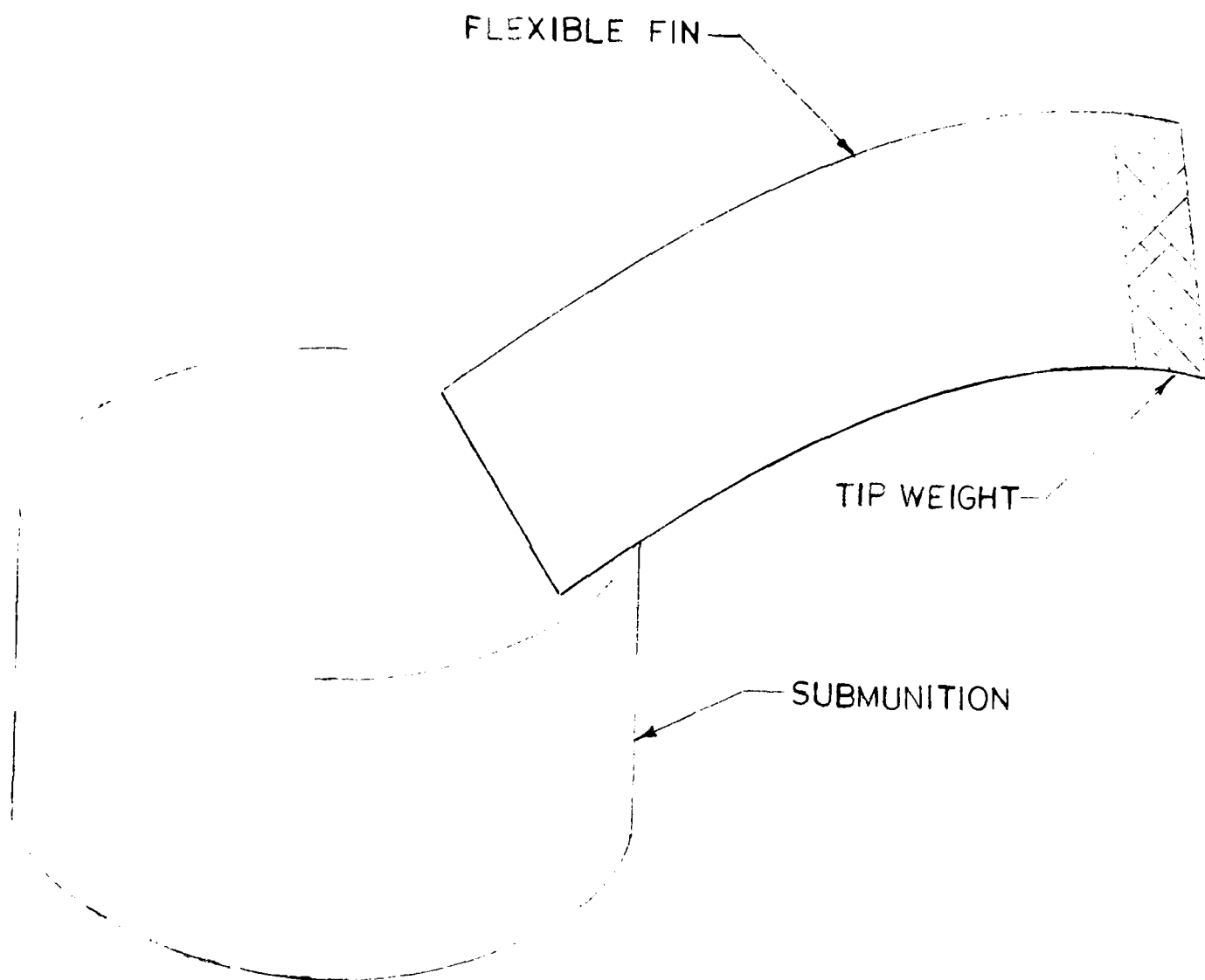


Figure 2. Submunition/flexible fin system

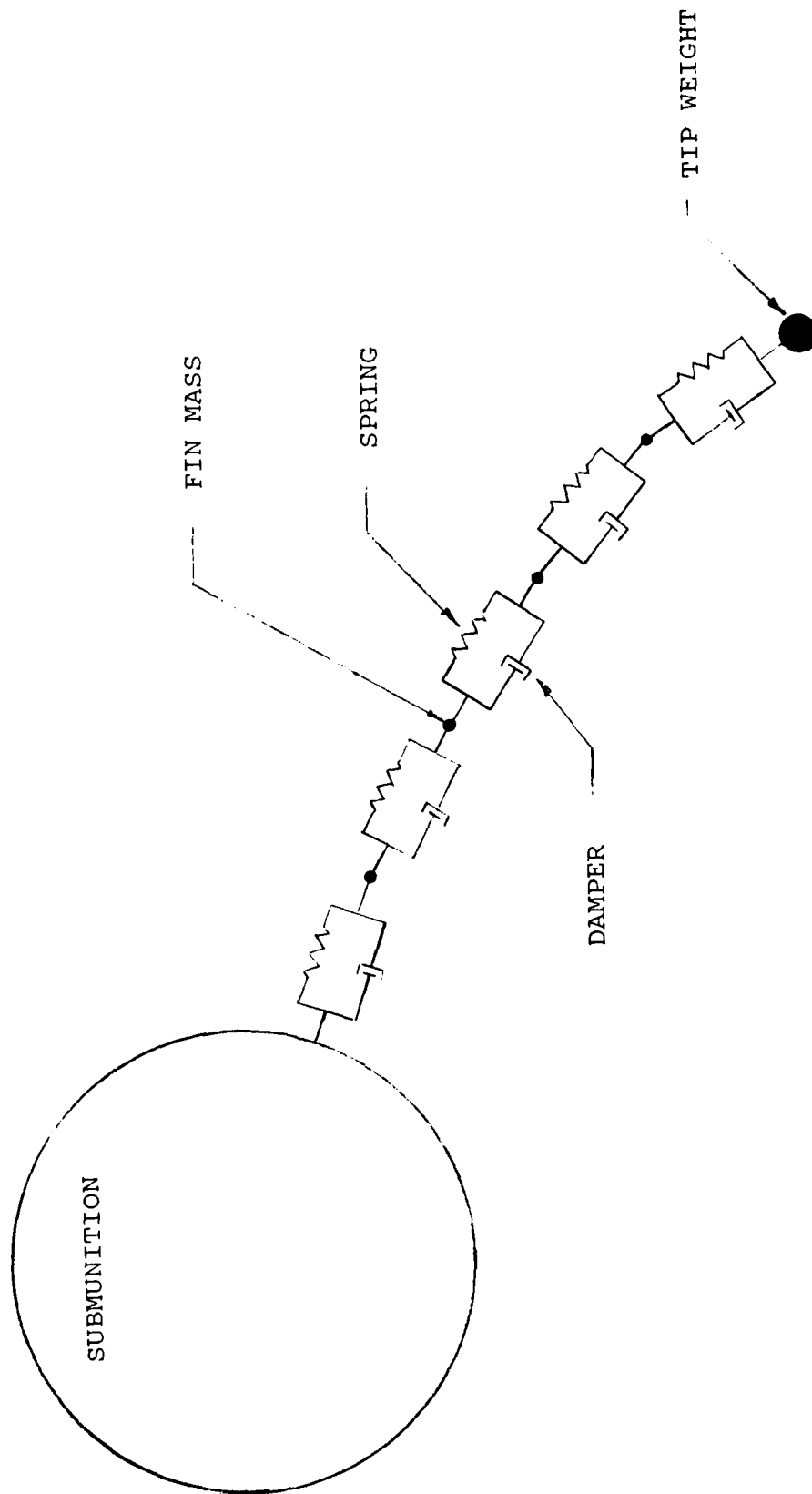


Figure 3. System model

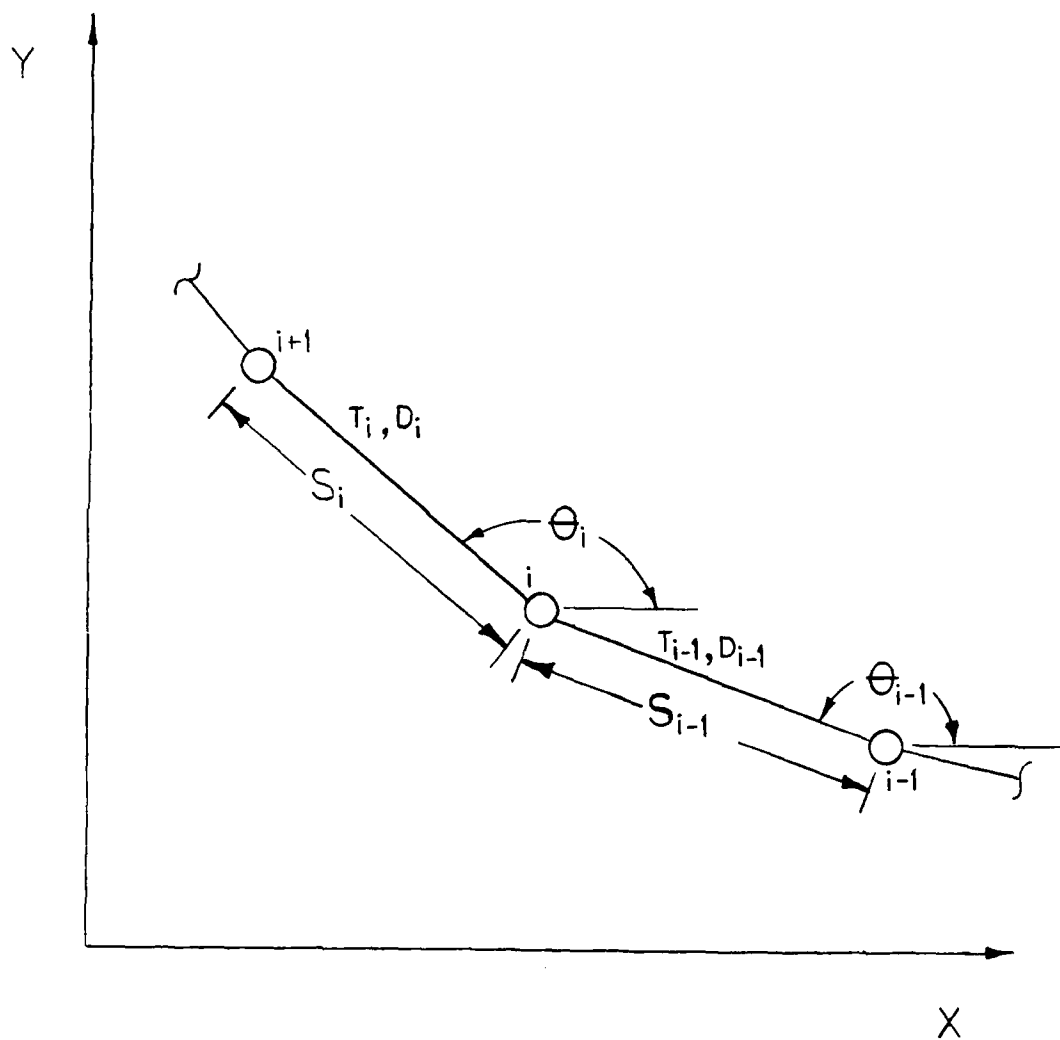


Figure 4. Simulation coordinate system

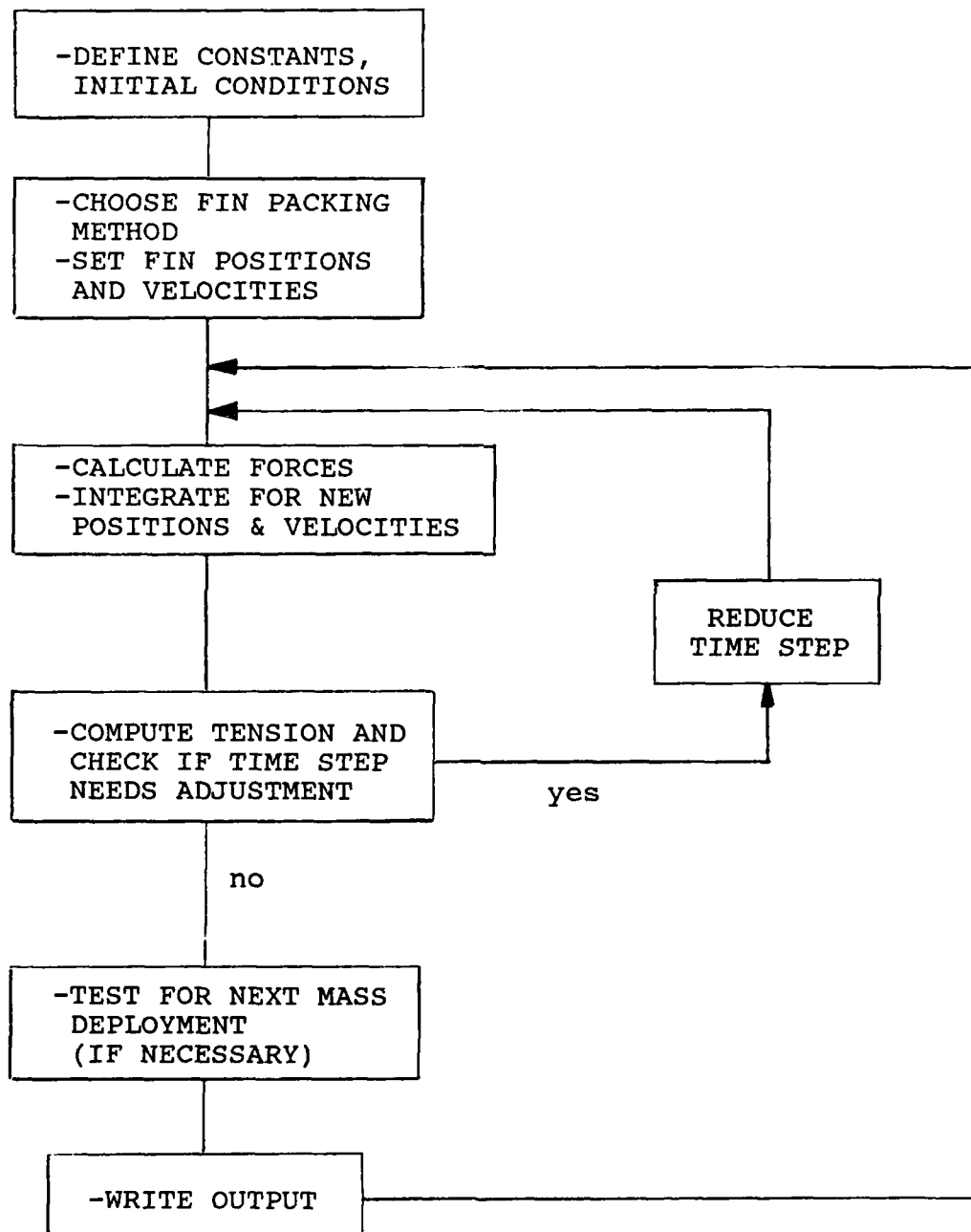


Figure 5. Simulation flowchart

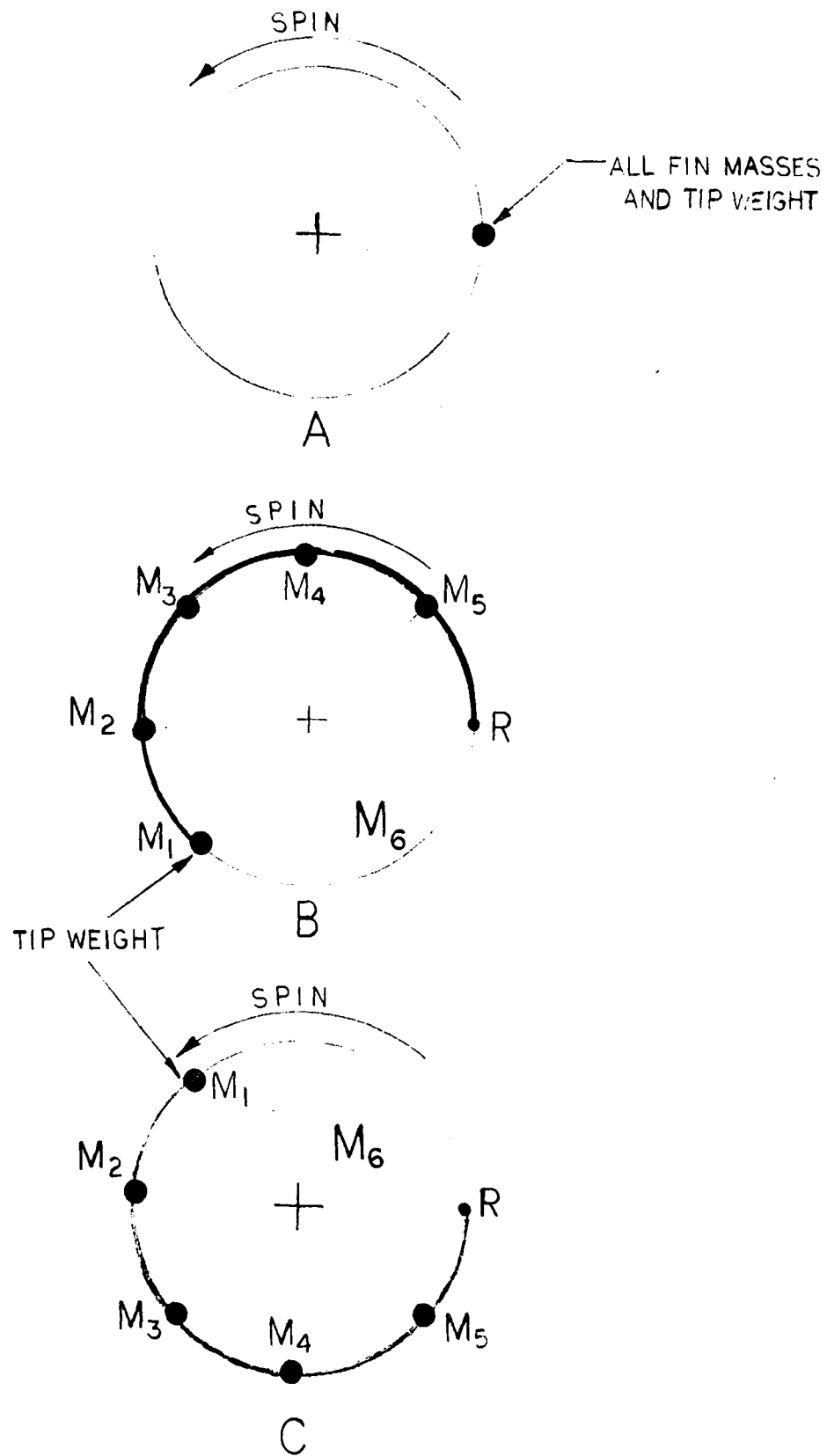


Figure 6. Simulated packing techniques

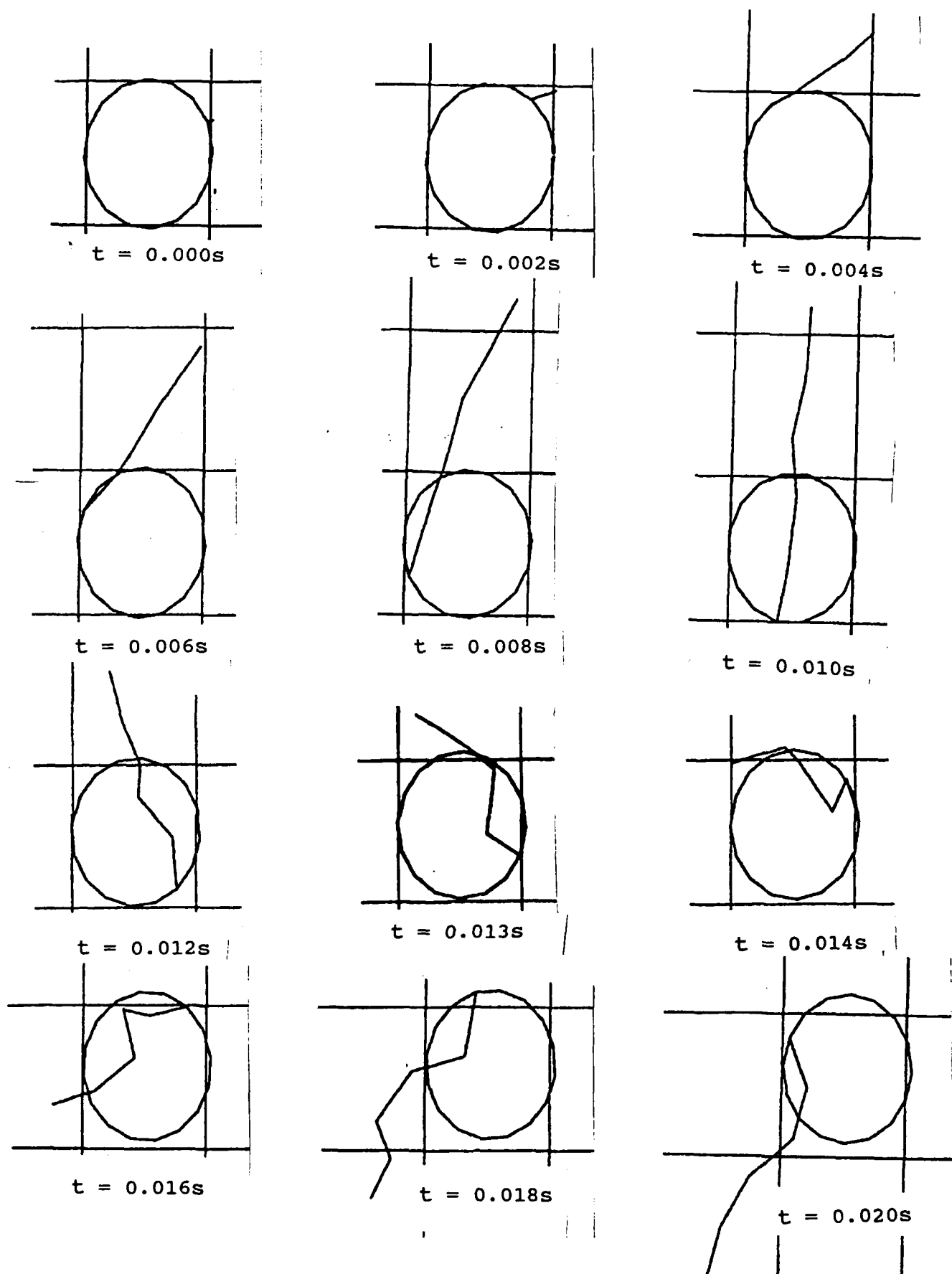


Figure 7. Deployment sequence, sequential deployment from root

## TENSION 1/2

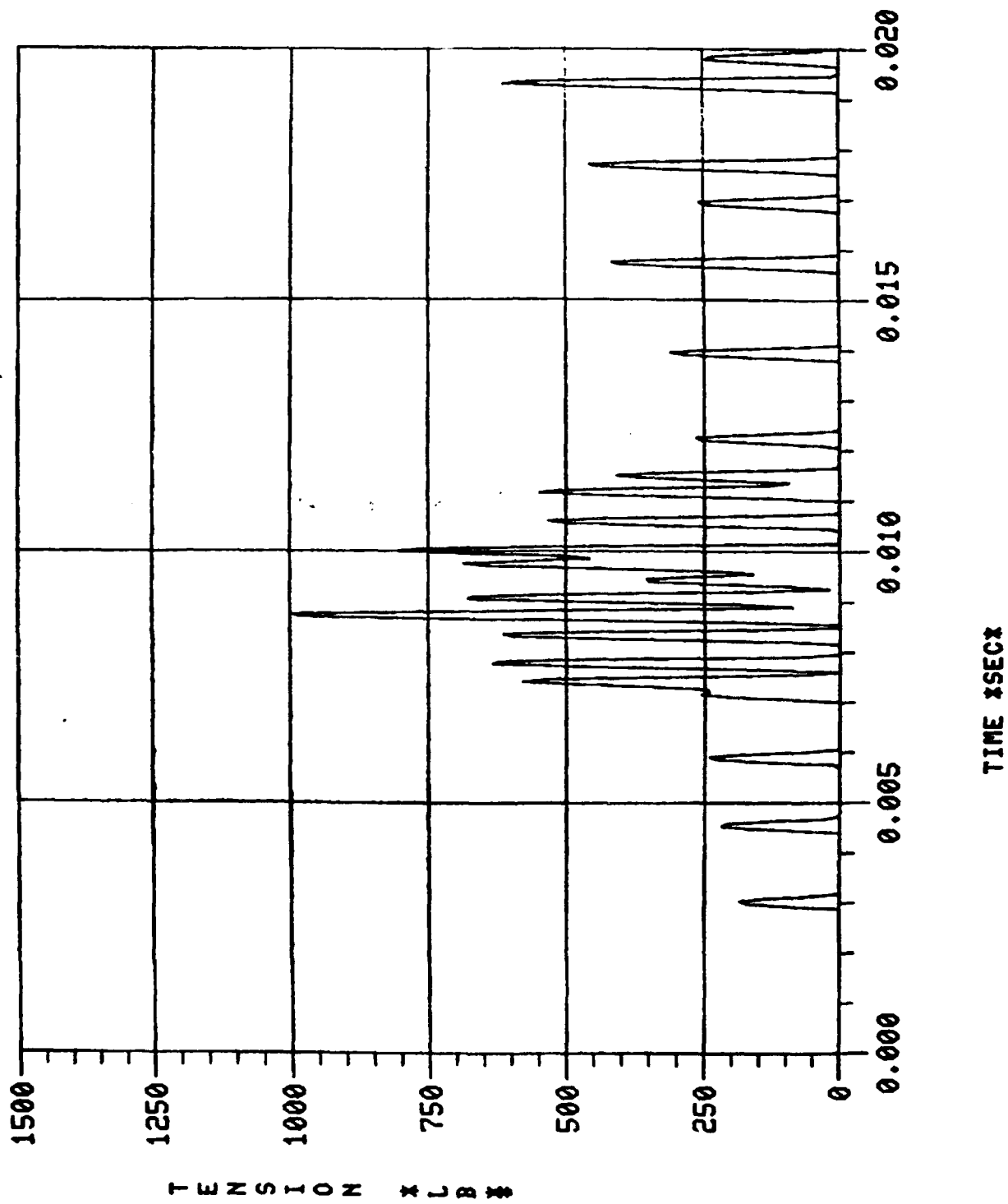
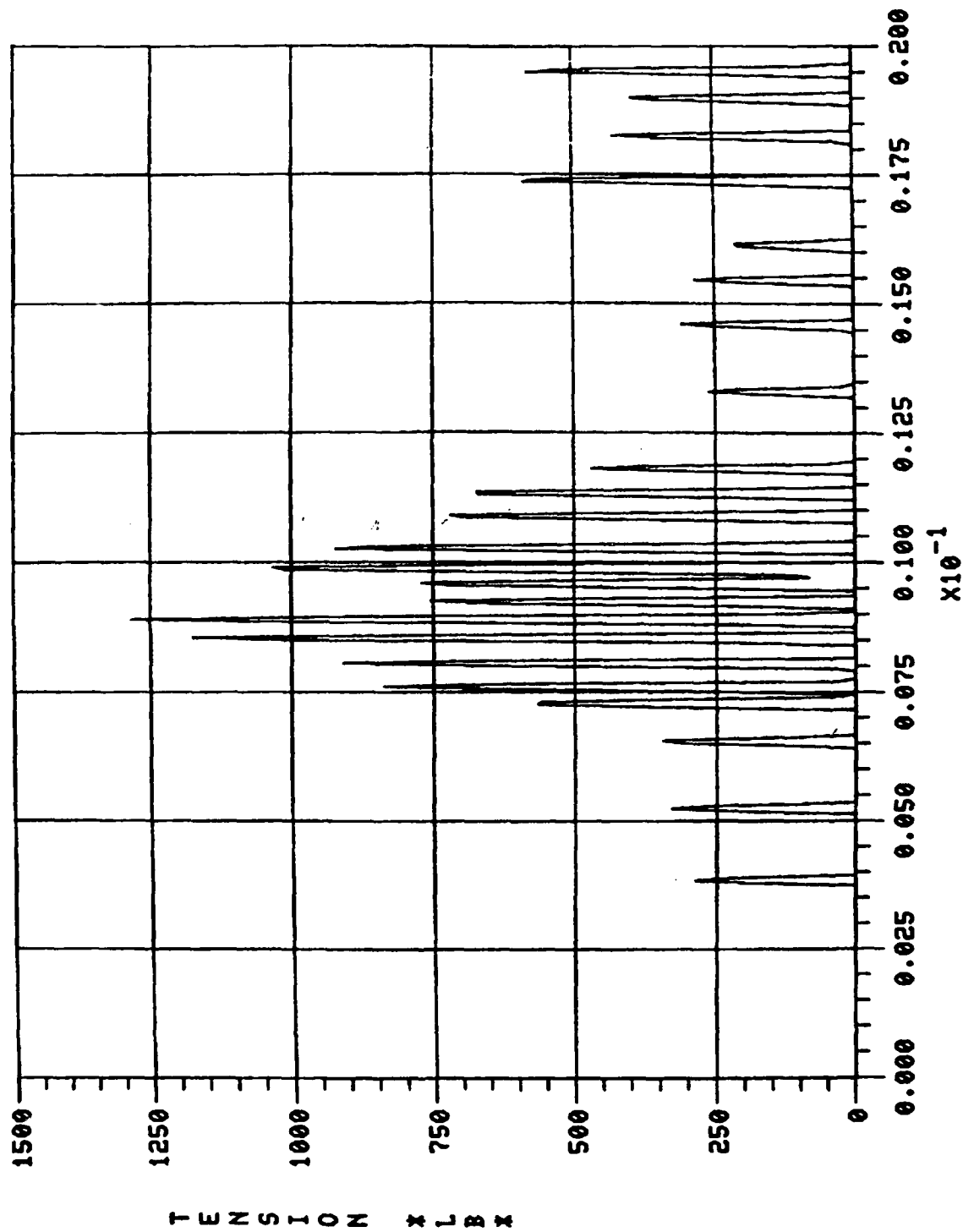


Figure 8. Tensions versus time for sequential deployment from root

91

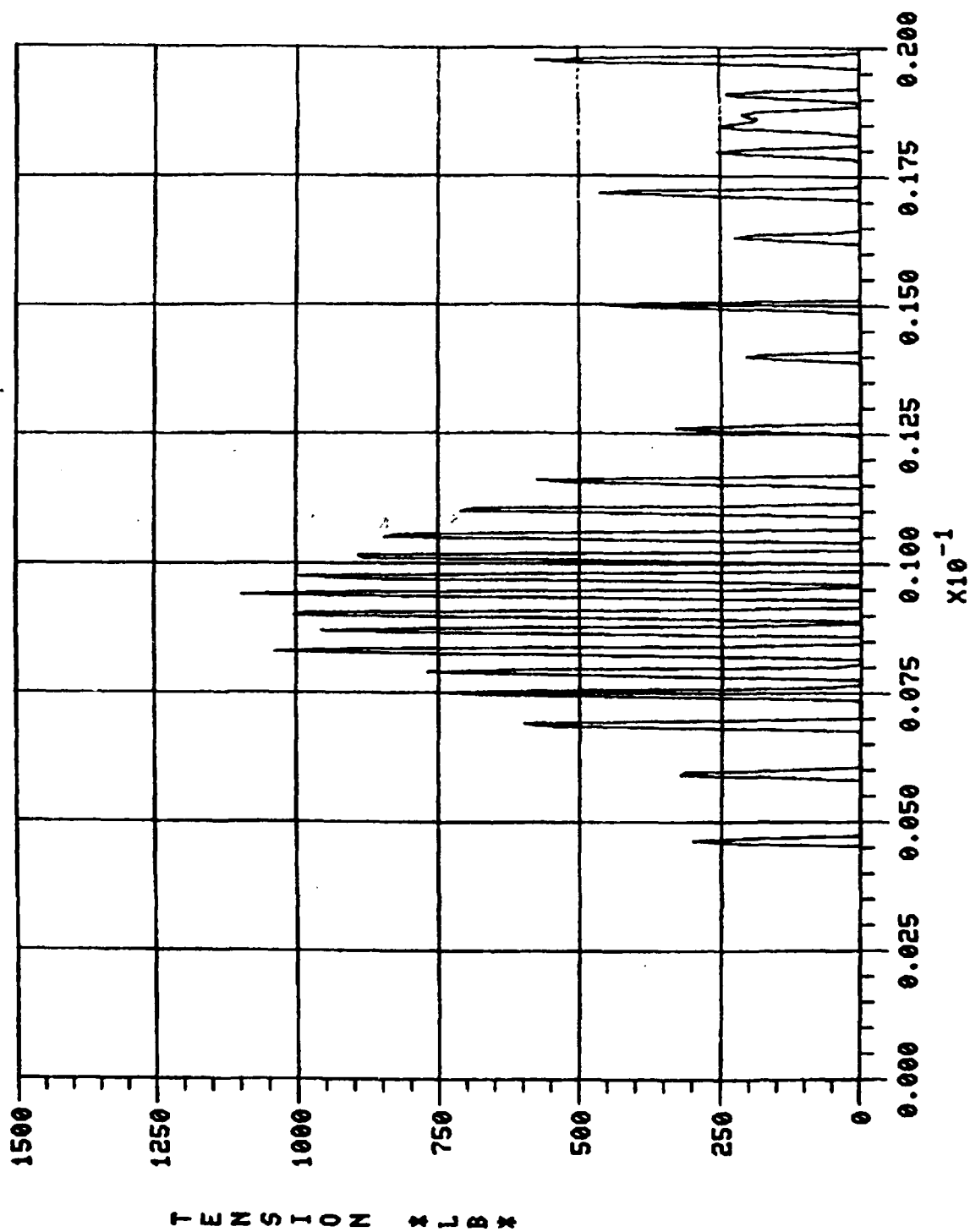
TENSION 2/3



TIME x SEC x

91

TENSION 3/4

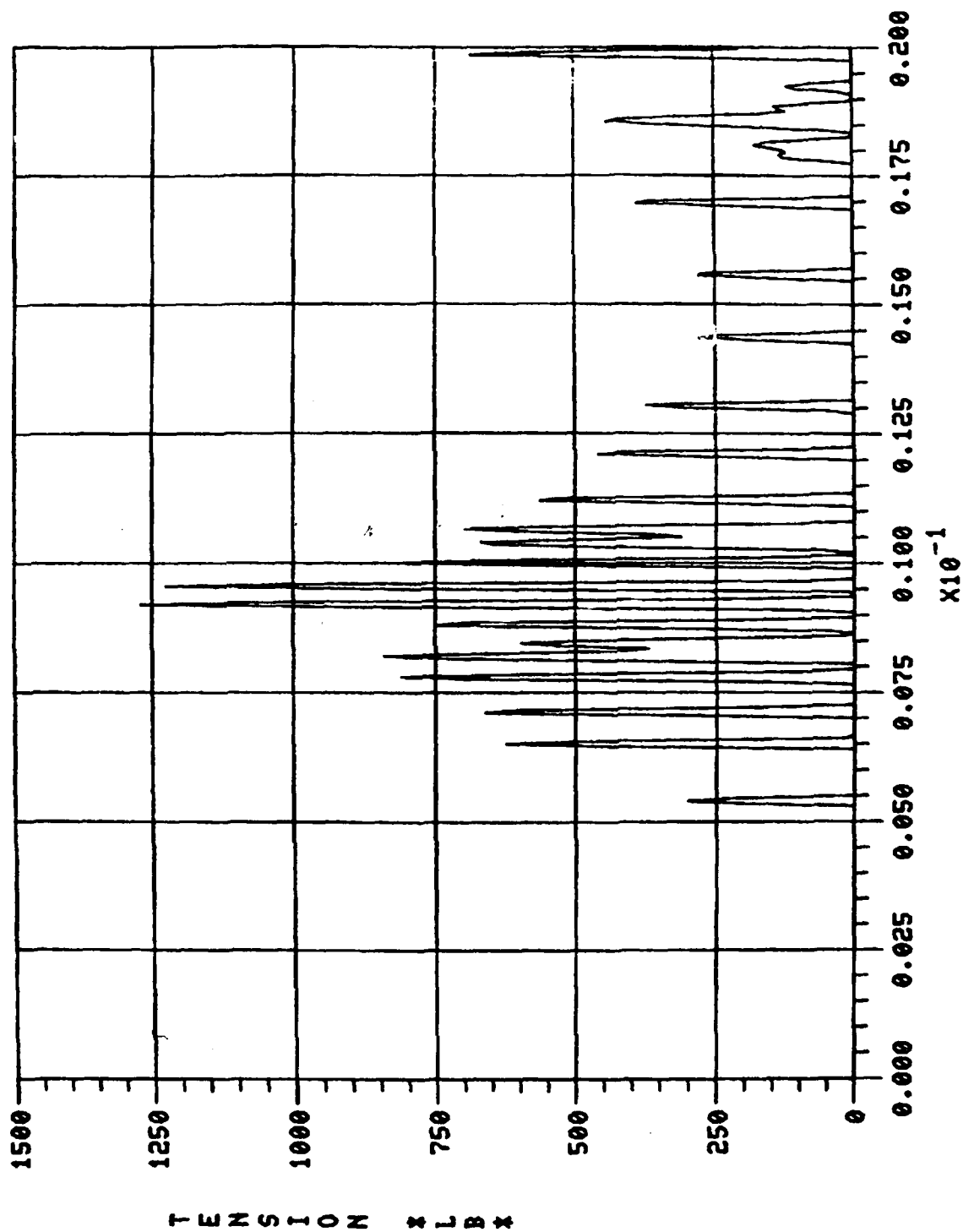


TENSION 3/4

Figure 8. (cont)

92

TENSION 4/5

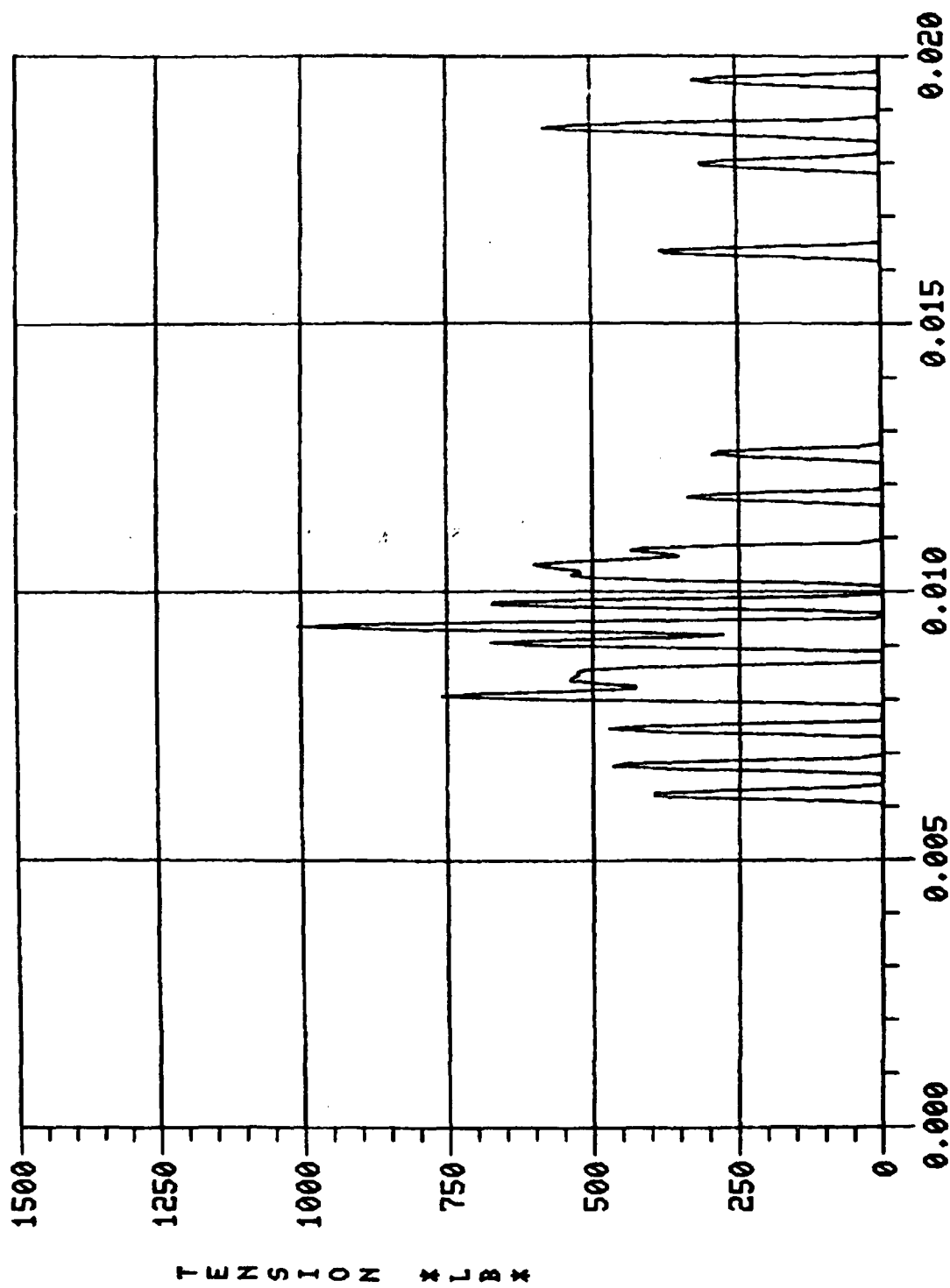


TIME x SEC x

Figure 8. (cont)

92

TENSION 5/ROOT



TIME \* SEC \*

Figure 8. (cont)

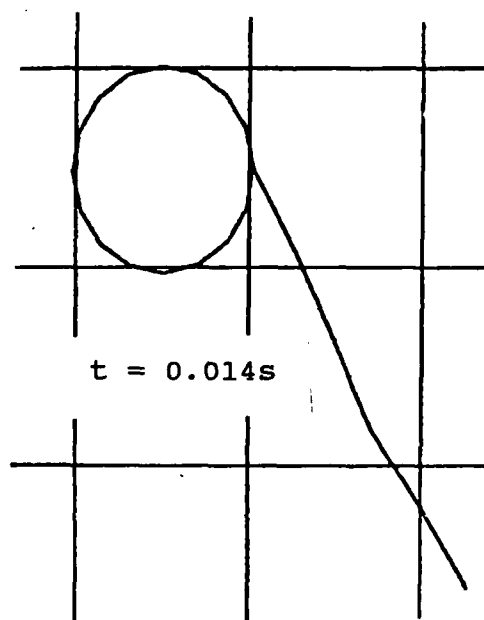
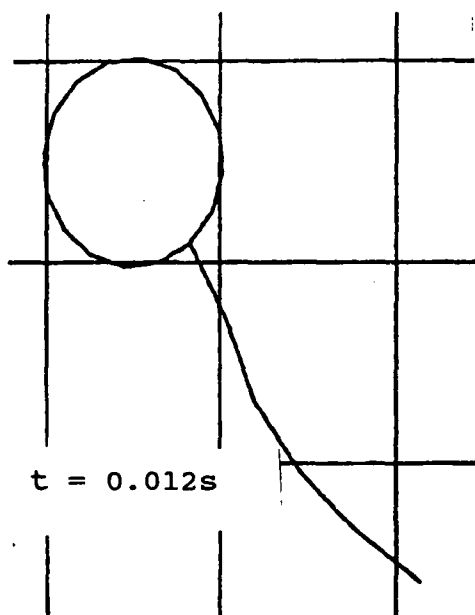
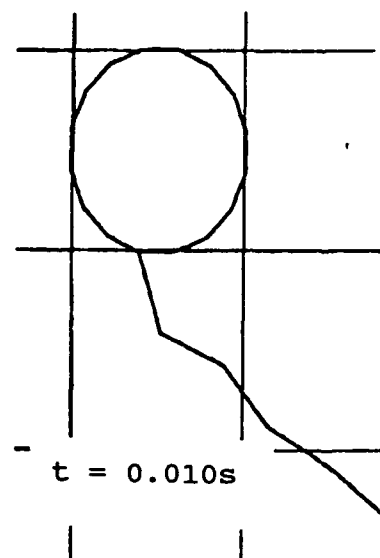
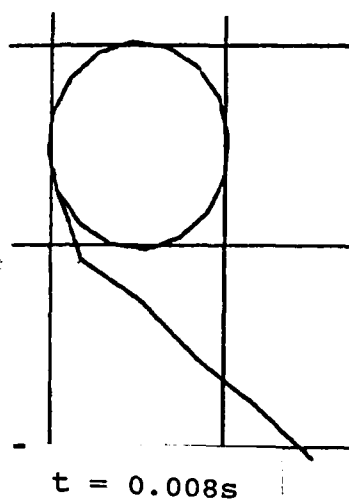
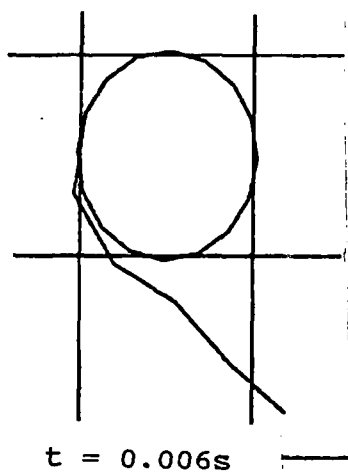
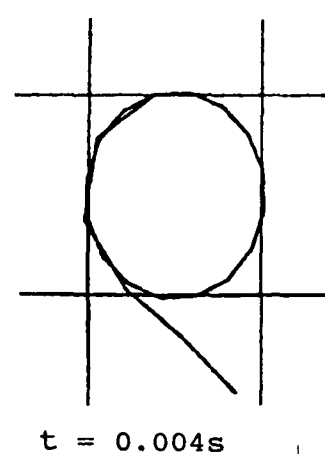
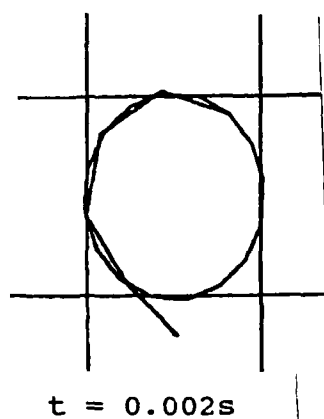
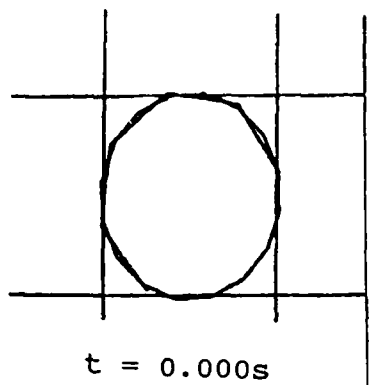


Figure 9. Deployment sequence, fin wrapped in spin direction

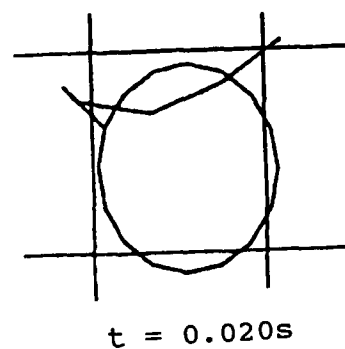
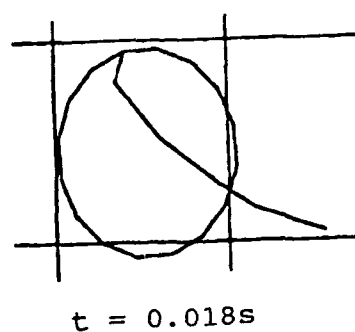
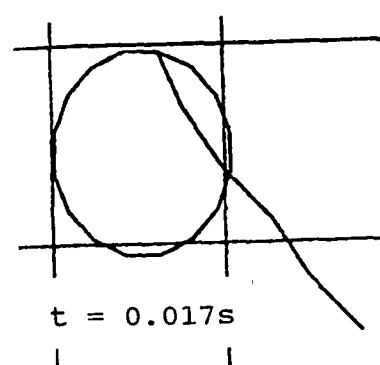
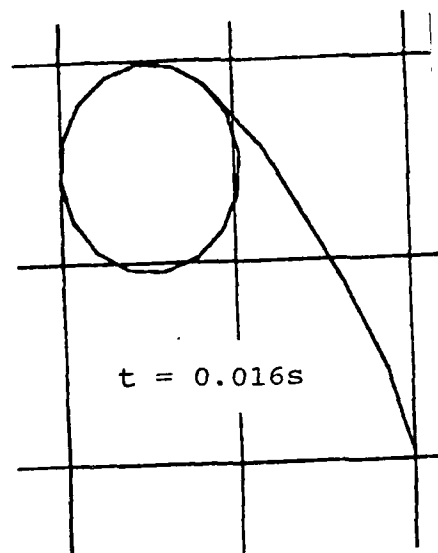


Figure 9. (cont)

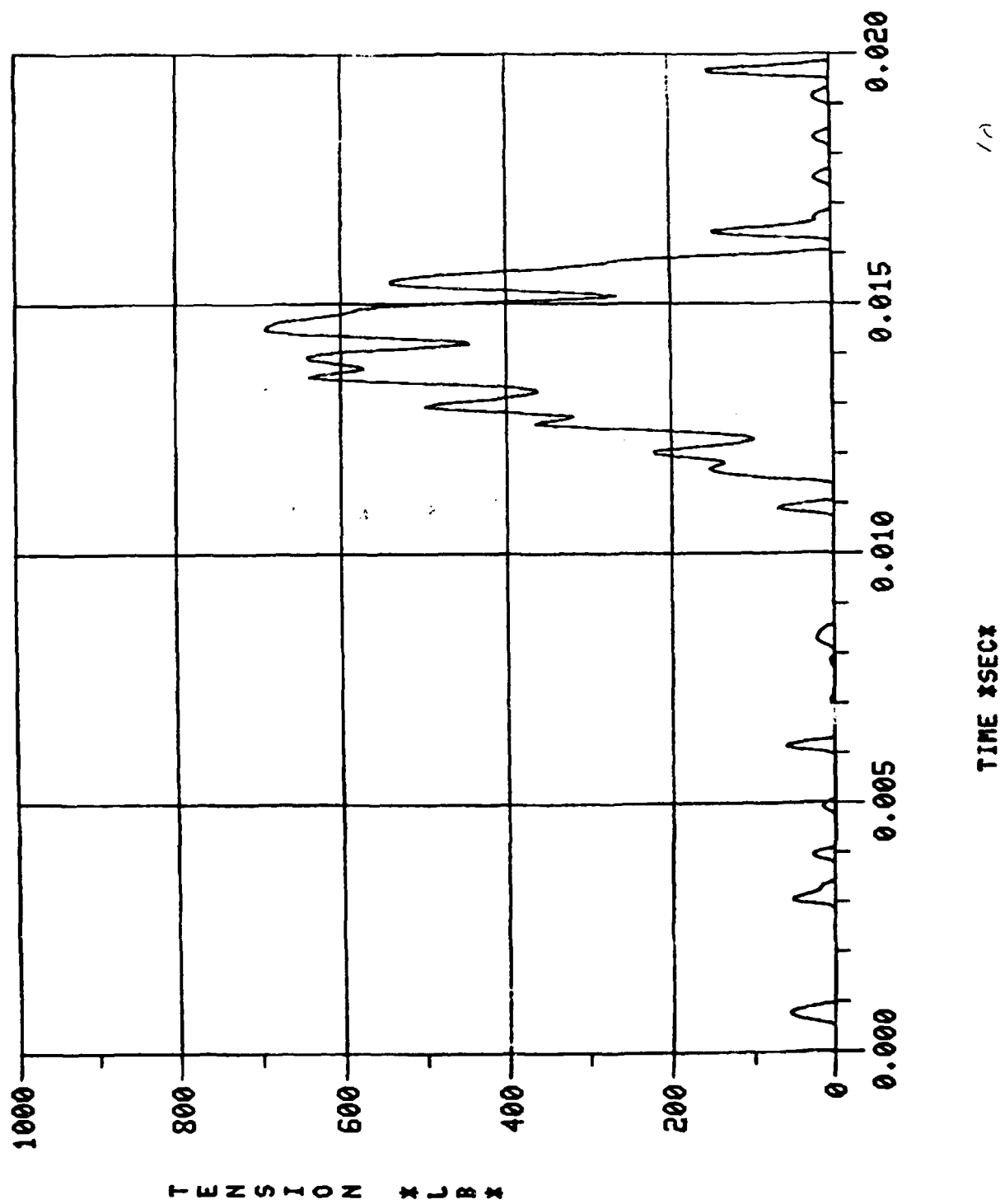
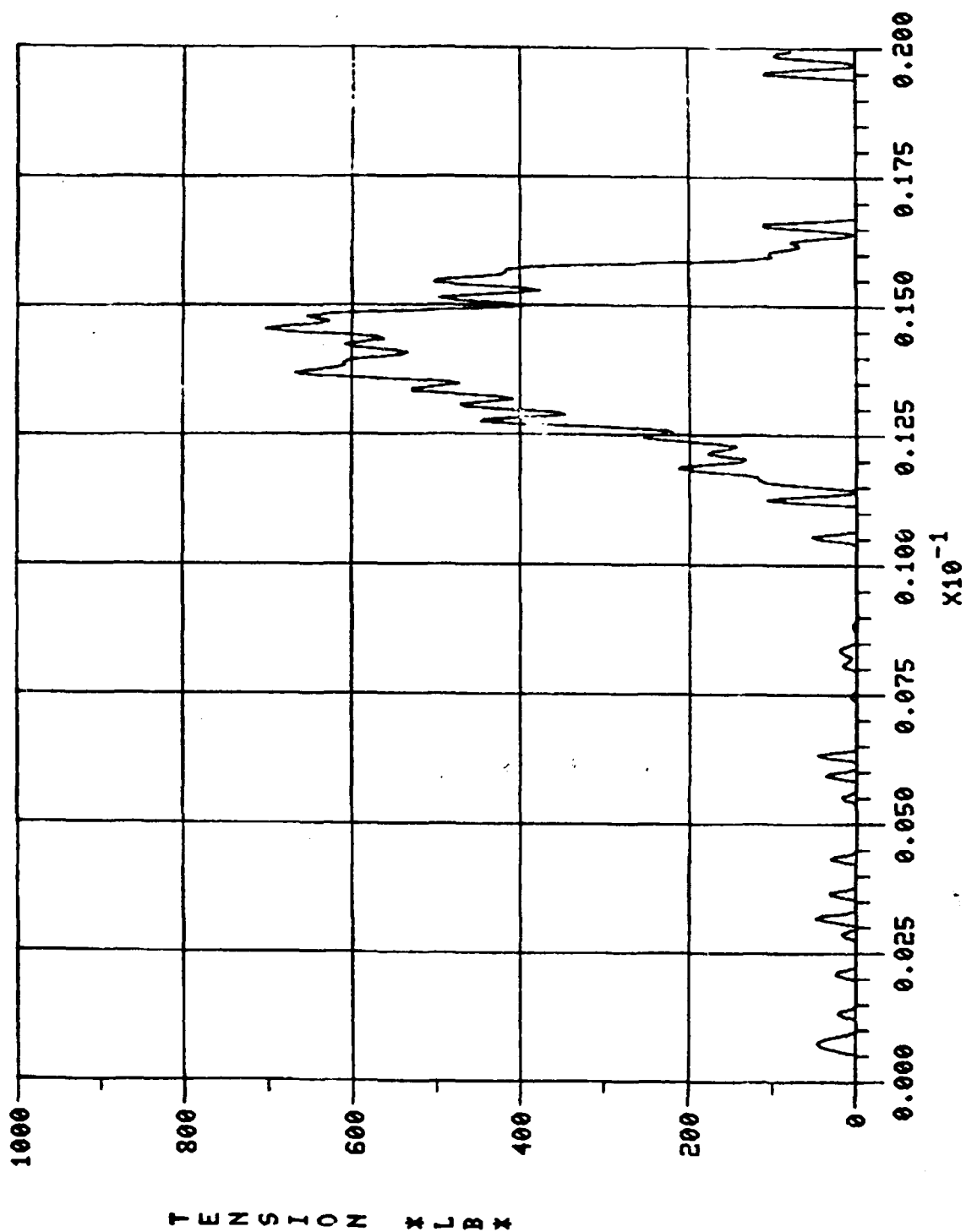


Figure 10. Tensions versus time for fin wrapped in spin direction

TENSION 2/3



/o

TIME x SEC x

Figure 10. (cont)

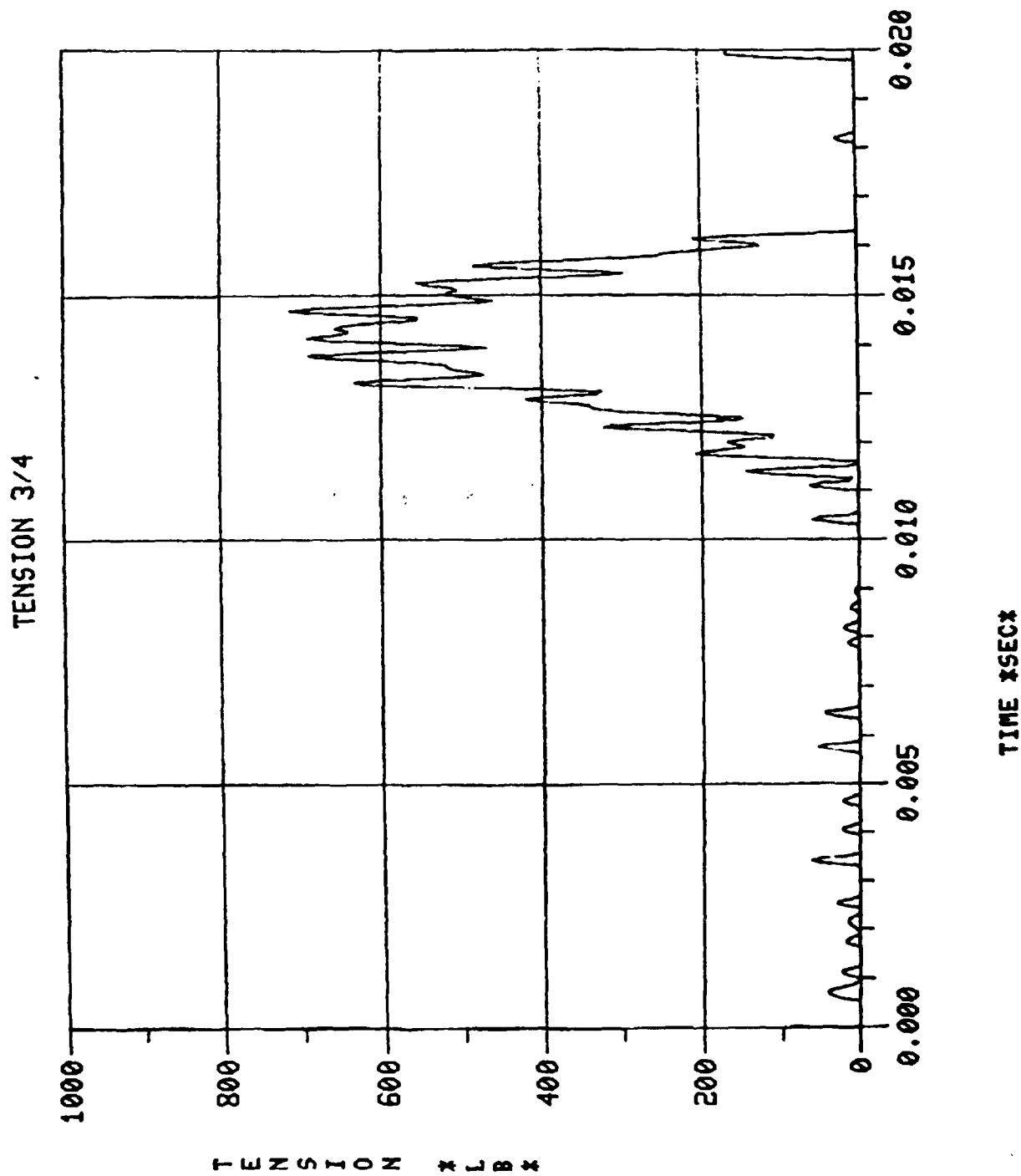
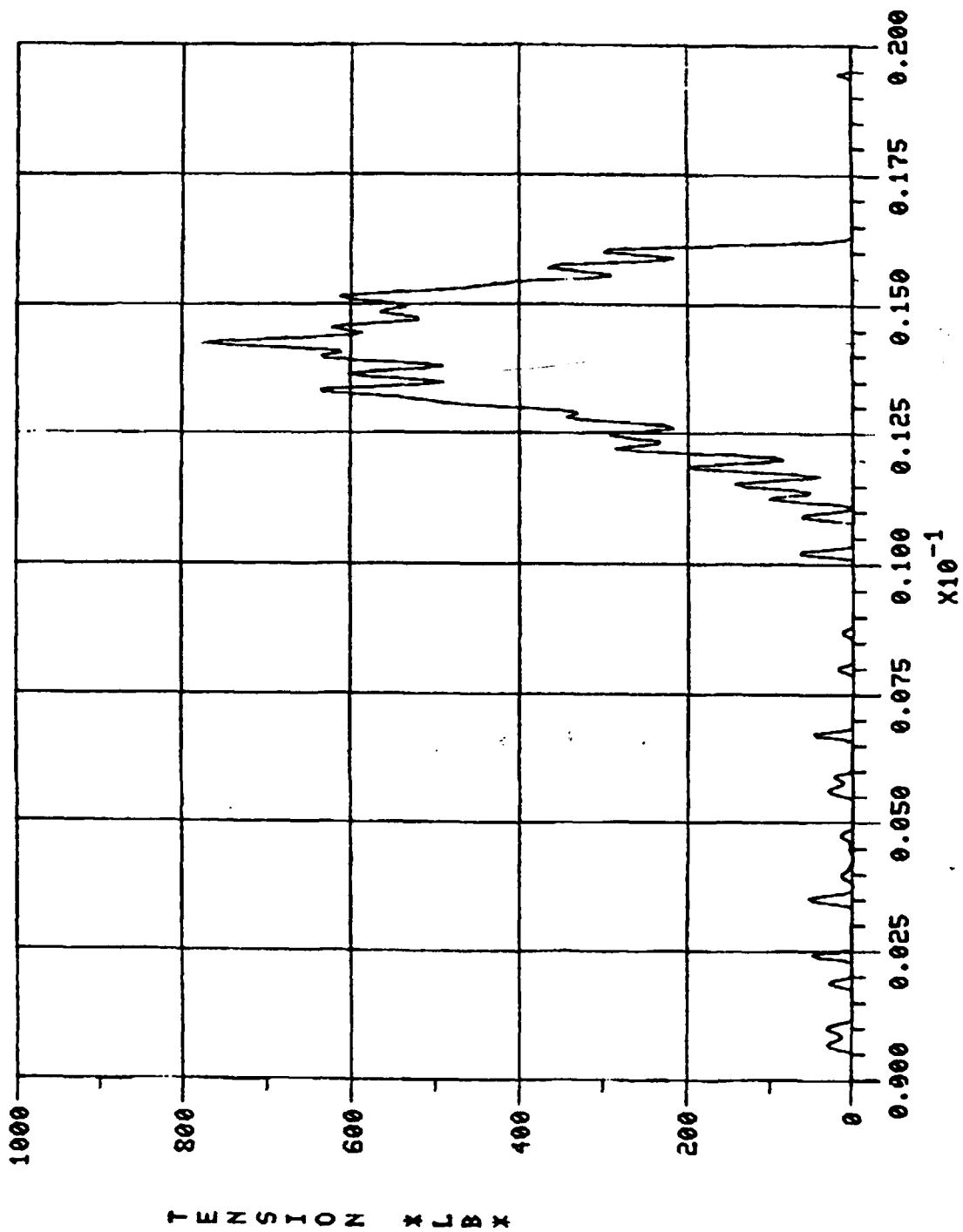


Figure 10. (cont)

TENSION 4/5



TIME x SECX

Figure 10. (cont)

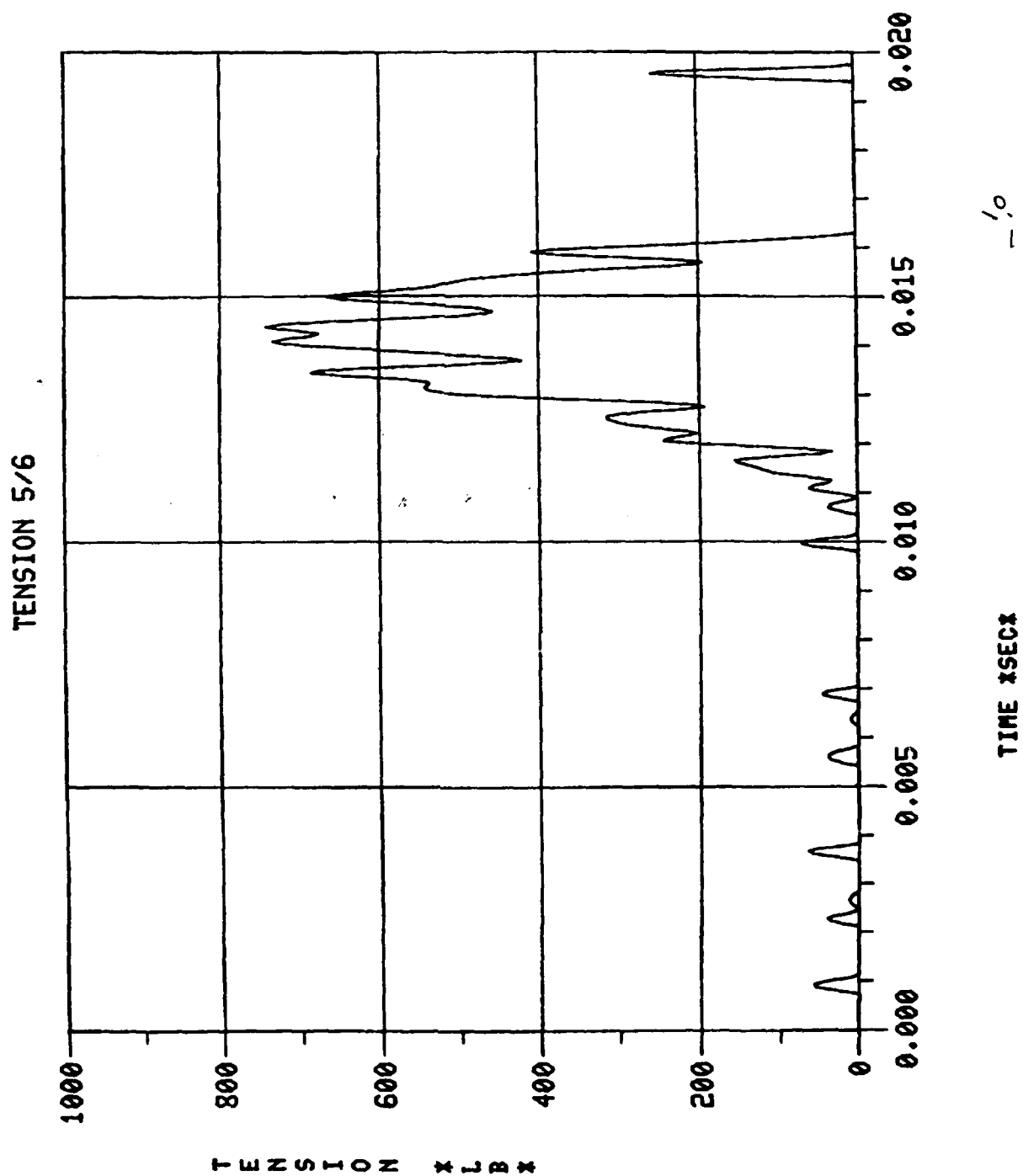


Figure 10. (cont)

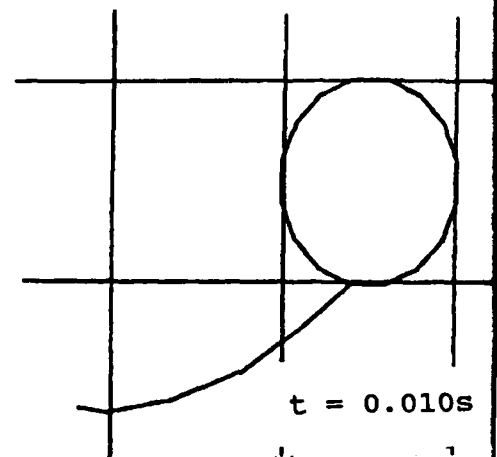
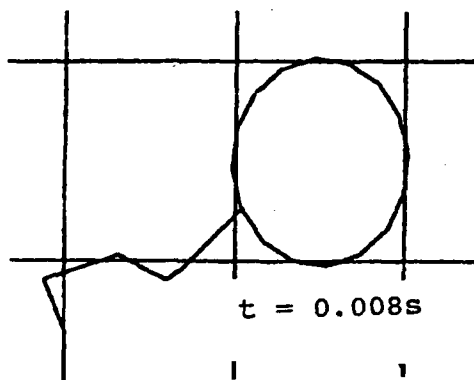
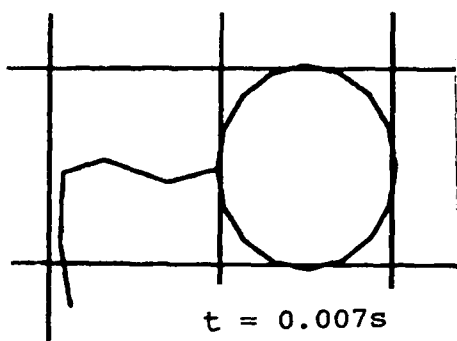
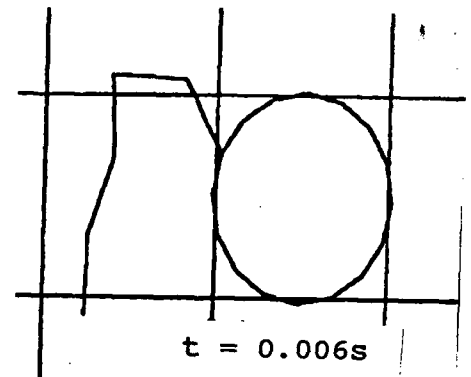
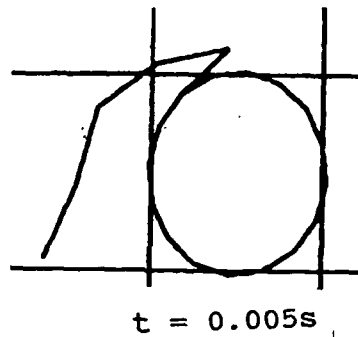
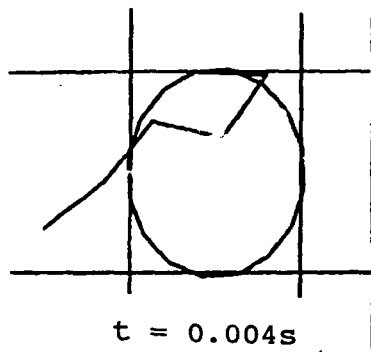
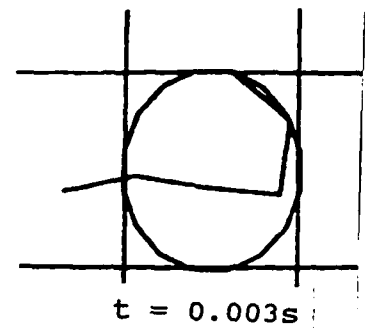
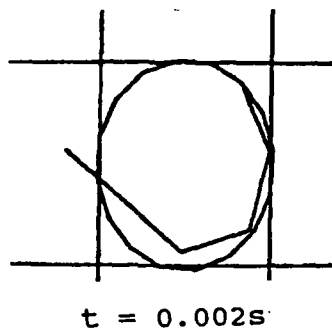
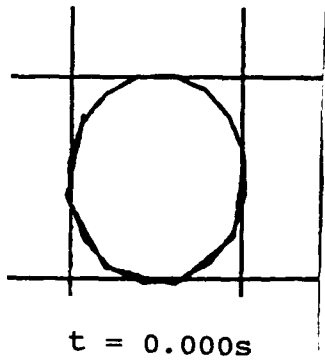


Figure 11. Deployment sequence, fin wrapped opposite to spin direction

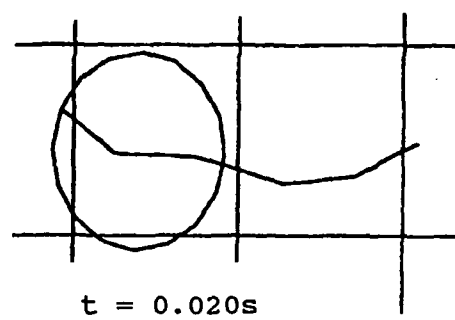
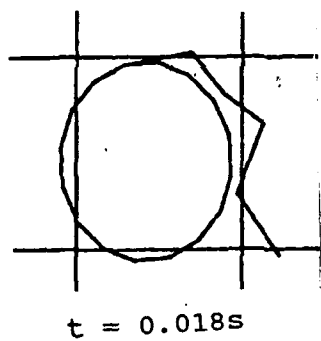
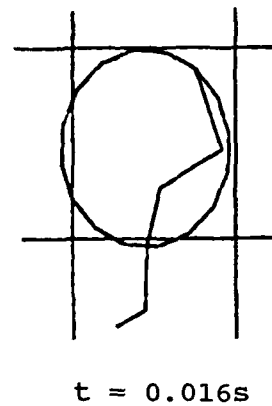
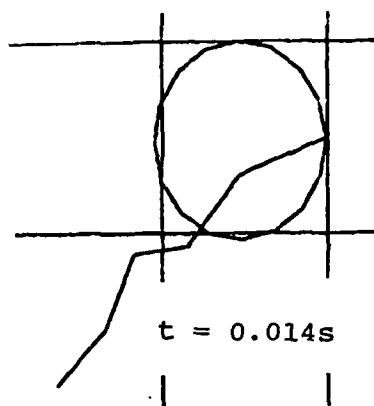
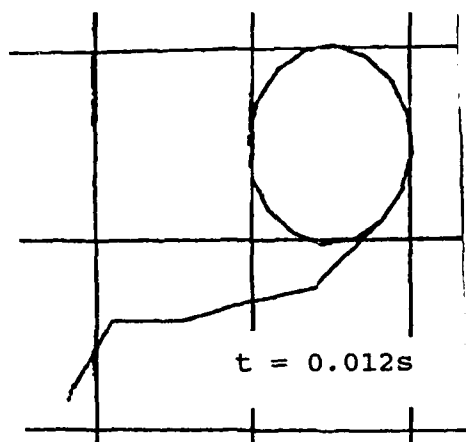


Figure 11. (cont)

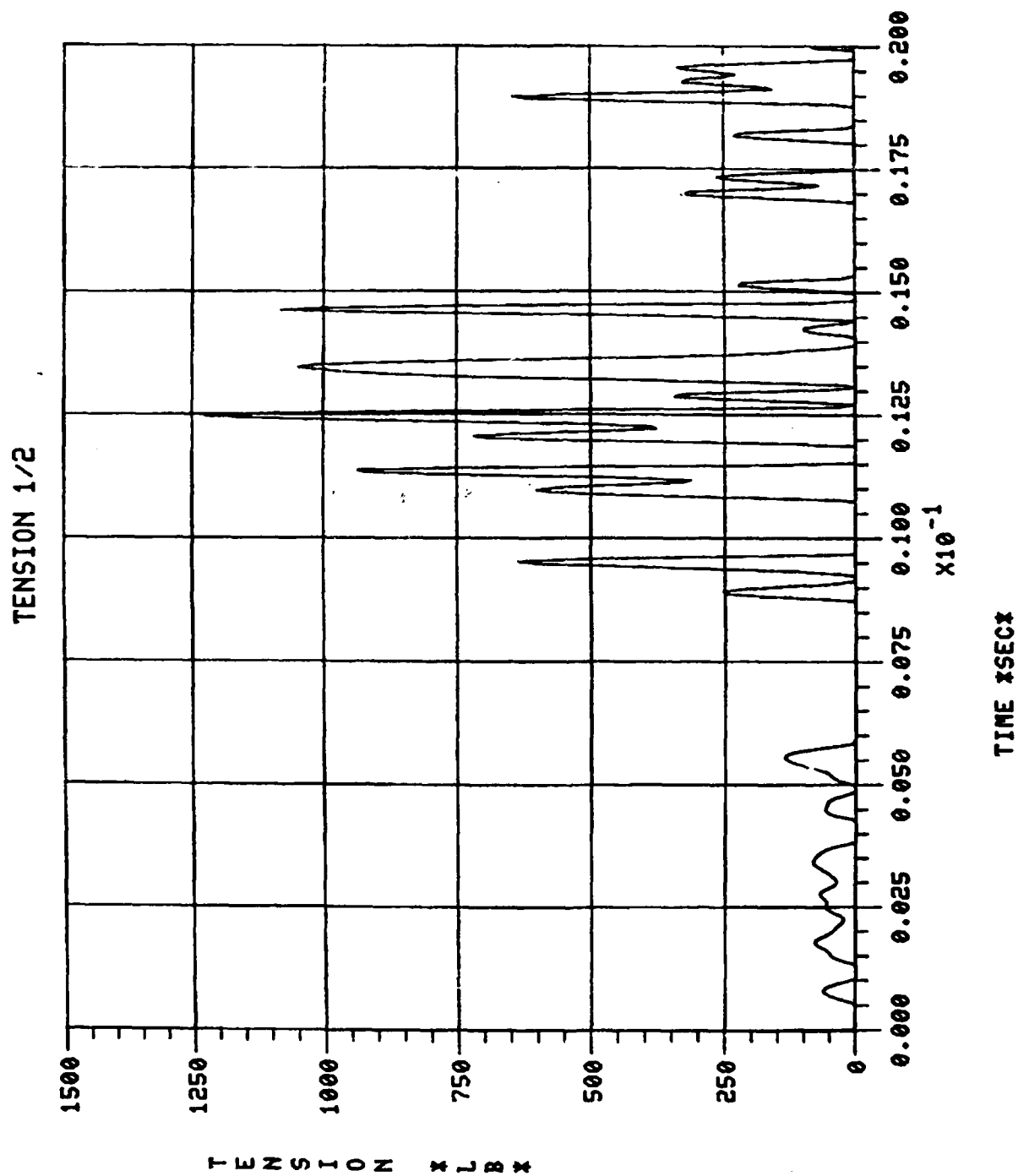


Figure 12. Tensions versus time for fin wrapped opposite to spin direction

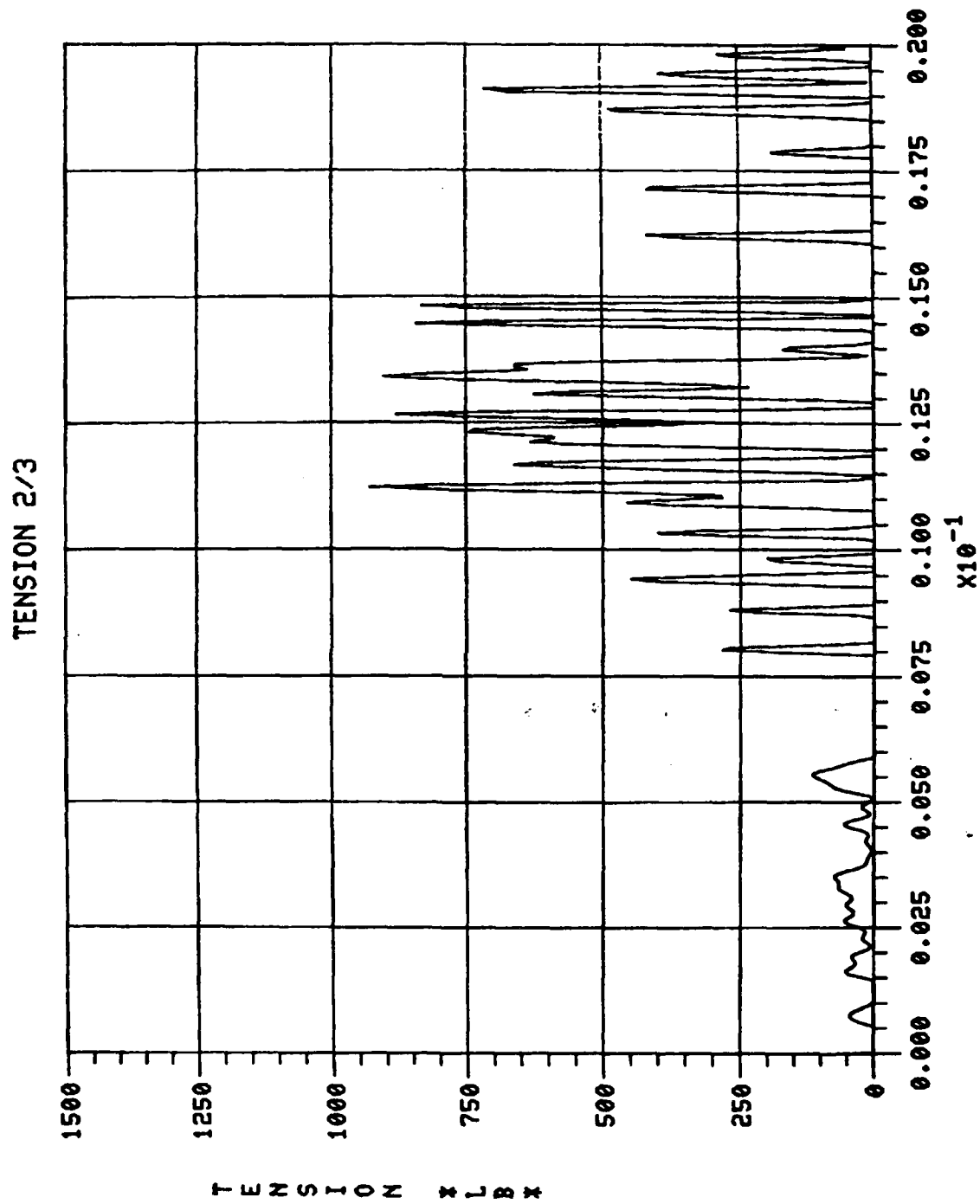
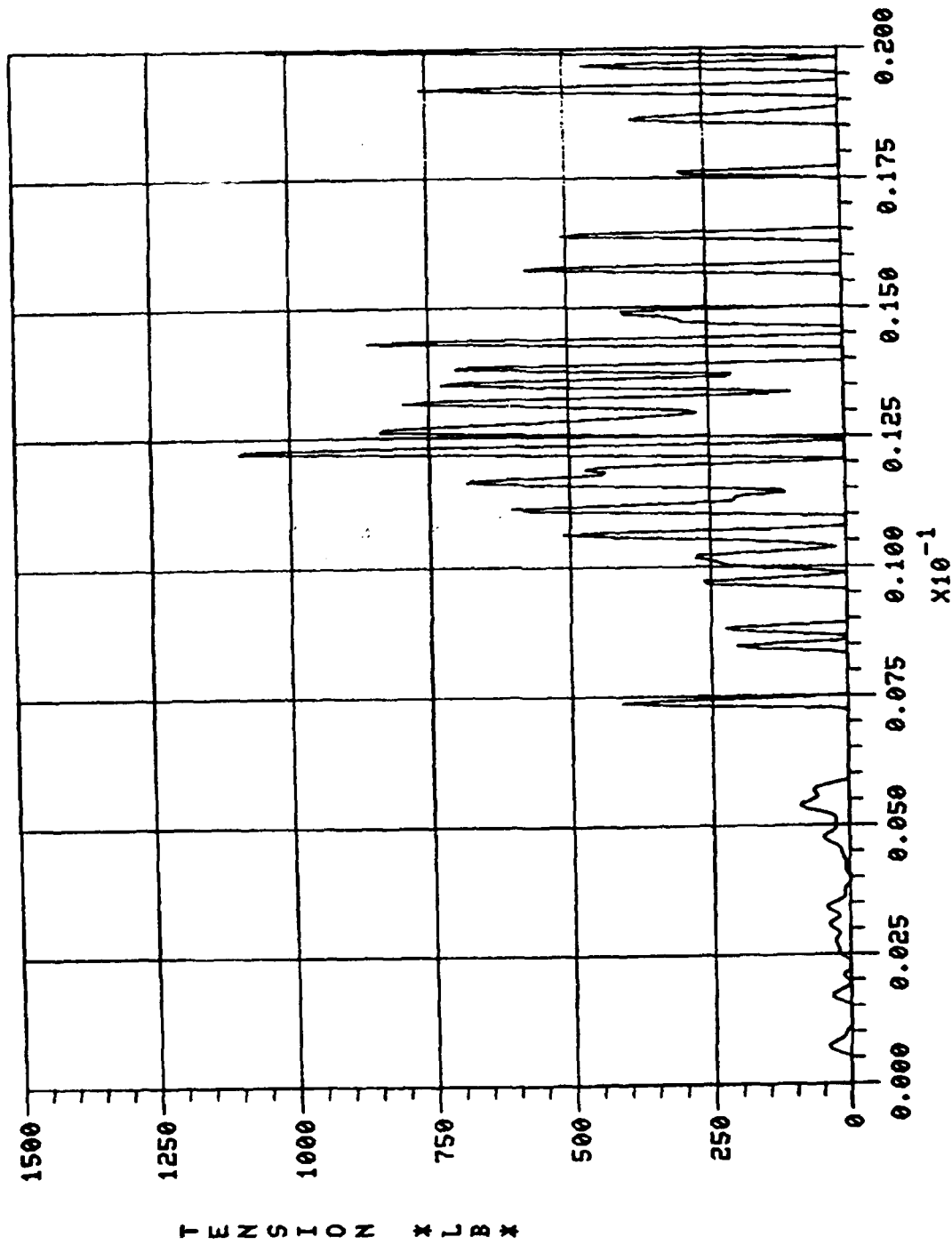


Figure 12. (cont)

TENSION 3/4



TIME \* SEC \*

Figure 12. (cont)

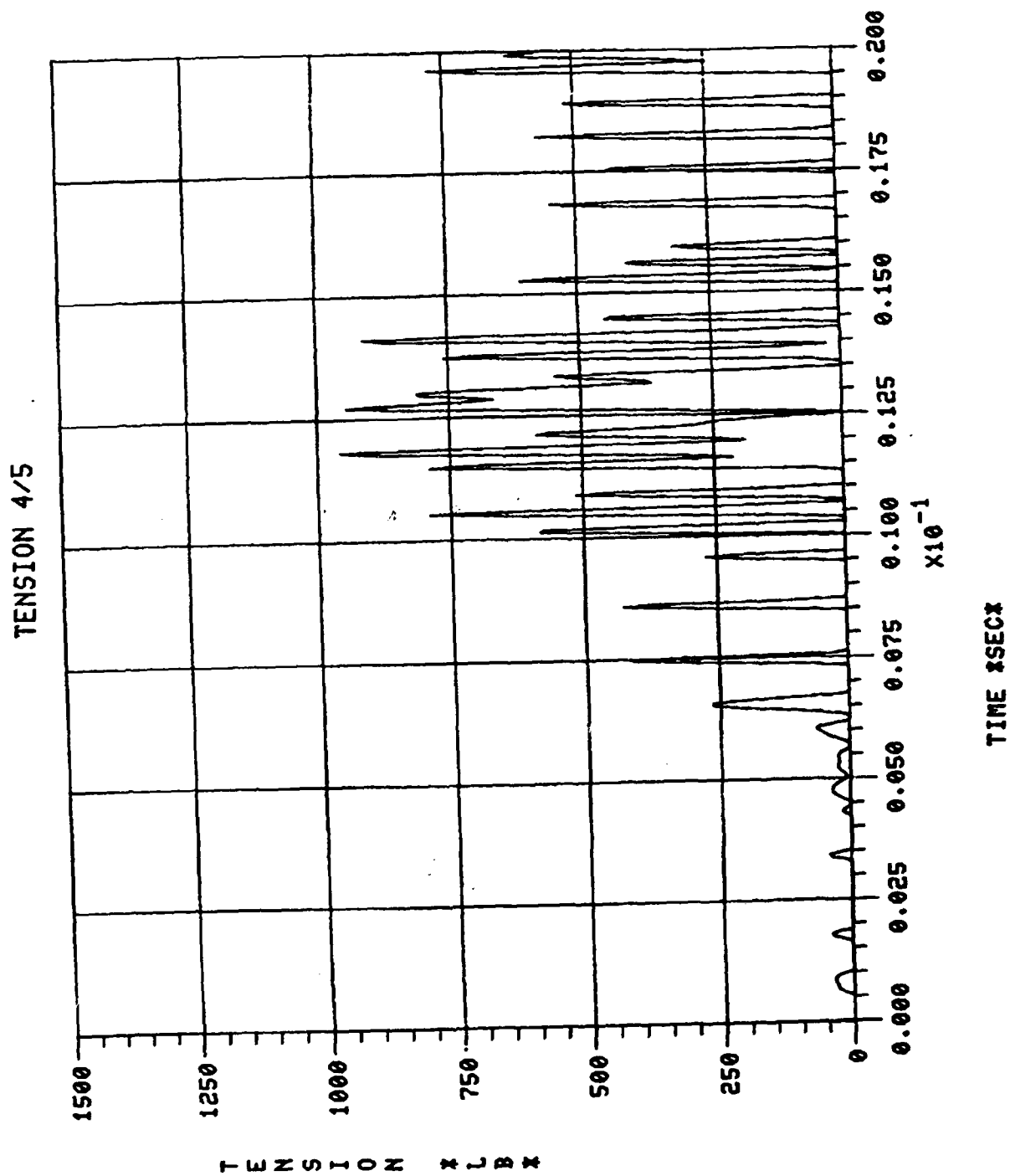
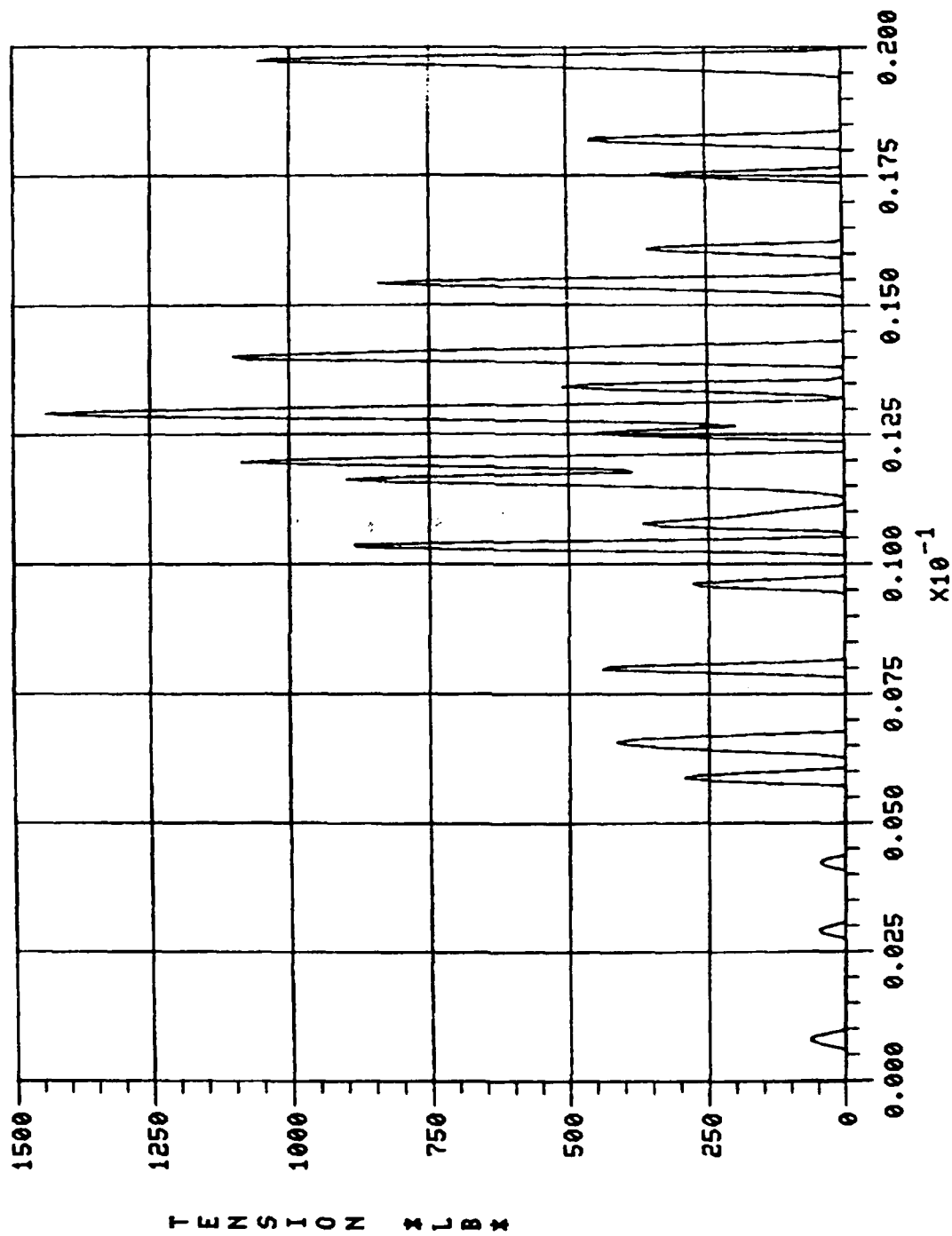


Figure 12. (cont)

TENSION 5/6



TIME x SEC x

Figure 12. (cont)

## REFERENCES

1. Koenig, W. H. and Kline, R. W., "Samara Type Decelerators," AIAA 8th Aerodynamic Decelerator and Balloon Technology Conference, Paper 84-0807, Hyannis, Massachusetts, April 1984.
2. Purvis, J. W., "Prediction of Parachute Line Sail During Lines First Deployment," Journal of Aircraft, Vol 20, Number 11, pp 940-945, November 1983.
3. Purvis, J. W., "Improved Prediction of Parachute Line Sail During Lines-First Deployment," AIAA 8th Aerodynamic Decelerator and Balloon Technology Conference, Paper 84-0786, Hyannis, Massachusetts, April 1984.

## GLOSSARY

$C_d$	Damping coefficient, lb/ft/s
$D_i$	Damping force between masses $i$ and $i_{i-1}$ , lb
$F_{Br}$	Breaking strength of fin material, lb
$k_{max}$	Maximum spring constant in system, lb/ft
$k$	Spring constant, lb/ft
$m_i$	Mass of element $i$ , lb
$m_{min}$	Minimum mass in the system, lb
$s_i$	Distance between mass $i$ and $i + 1$ , ft
$s_{o_i}$	Unstretched distance between mass $i$ and $i + 1$ , ft
$T_i$	Tension between mass $i$ and $i + 1$ , lb
$x_i, y_i$	Coordinates of mass $i$ , ft
$\theta_i$	Angle (with respect to horizontal) of line segment connection mass $i$ and $i + 1$ , deg
$w_{max}$	Maximum frequency in system, rad/s

APPENDIX

CLOSED FORM SOLUTION OF SIMPLE TWO BODY PROBLEM

Two bodies of mass  $m_1$  and  $m_2$  are connected by a massless spring of free length  $l$  and spring constant  $K$  (fig. A1). Free body diagrams of the masses are also shown. The equations of motion of the two bodies (assuming no damping) are:

$$m_1 \ddot{x}_1 = k(x_2 - x_1 - l) \quad (A1)$$

$$m_2 \ddot{x}_2 = -k(x_2 - x_1 - l) \quad (A2)$$

These equations can be rewritten as:

$$\ddot{x}_1 + w_1^2 x_1 = w_1^2 (x_2 - l) \quad (A3)$$

$$\ddot{x}_2 + w_2^2 x_2 = w_2^2 (x_2 + l) \quad (A4)$$

where

$$w_{1,2} = \sqrt{\frac{k}{m_{1,2}}}$$

Introduce a differential operator  $P$  into equation (A1):

$$P^2 x_1 + w_1^2 x_1 = w_1^2 (x_2 - l) \quad (A5)$$

solve for  $x_1$ :

$$x_1 = \frac{w_1^2 (x_2 - l)}{(P^2 + w_1^2)} \quad (A6)$$

Substitute equation (A6) into equation (A4):

$$\ddot{x}_2 + w_2^2 x_2 = w_2^2 \left[ \frac{w_1^2 (x_2 - l)}{(P^2 + w_1^2)} + l \right] \quad (A7)$$

Equation (A7) can be simplified to:

$$\ddot{\ddot{x}}_2 + (w_1^2 + w_2^2) \ddot{x}_2 = 0 \quad (A8)$$

Define  $y = \ddot{x}_2$  and  $w^2 = w_1^2 + w_2^2$  so

$$\ddot{y} + w^2 y = 0 \quad (A9)$$

The solution of equation (A9) is of the form

$$y = A \sin wt + B \cos wt \quad (A10)$$

Since  $y = \ddot{x}_2$

$$\ddot{x}_2 = A \sin wt + B \cos wt \quad (A11)$$

Integrating once

$$\dot{x}_2 = -A/w \cos wt + B/w \sin wt + C \quad (A12)$$

Integrating again

$$x_2 = -A/w^2 \sin wt - B/w^2 \cos wt + ct + D \quad (A13)$$

Initial conditions may now be used to determine the constants A, B, C, and D. For the test case, assume  $x_1(0) = 0$ ,  $x_2(0) = l$ ,  $\dot{x}_1(0) = 0$ , and  $\dot{x}_2(0) = V_0$ . Substituting for  $x_1(0)$  and  $x_2(0)$  in equation (A2),  $\ddot{x}_2(0) = 0$ . If  $\ddot{x}_2(0) = 0$ , from equation (A11),  $B = 0$ . So far the solution is:

$$x_2 = -A/w^2 \sin wt + ct + D \quad (A14)$$

Since  $x_2(0) = l$ , from (A14),  $D = l$ . If

$$\ddot{x}_2 = A \sin wt \quad (A15)$$

then

$$\ddot{x}_2 = Aw \cos wt \quad (A16)$$

From equation (A2),

$$\ddot{x}_2 = -w_2^2(x_2 - x_1 - l) \quad (A17)$$

so

$$\ddot{x}_2 = -w_2^2(\dot{x}_2 - \dot{x}_1) \quad (A18)$$

Equating equations (A16) and (A18):

$$Aw \cos wt = -w_2^2(\dot{x}_2 - \dot{x}_1) \quad (A19)$$

Substituting for  $\dot{x}_1(0)$  and  $\dot{x}_2(0)$

$$A = \frac{-w_2^2}{w} V_o \quad (A20)$$

Finally, substituting  $\dot{x}_2(0)$  into equation (A12)

$$V_o = \frac{w_2^2}{w^2} V_o + c \quad (A21)$$

so

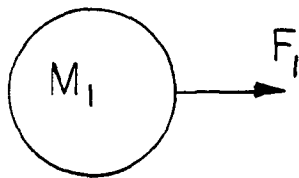
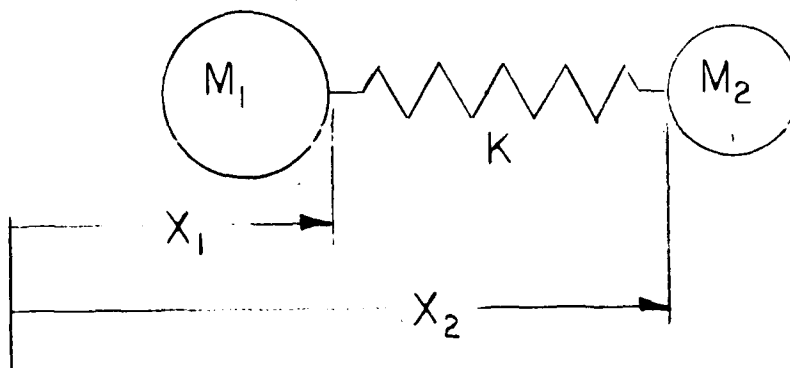
$$c = V_o \left(1 - \frac{w_2^2}{w^2}\right) \quad (A22)$$

The solution of equation (A8) is:

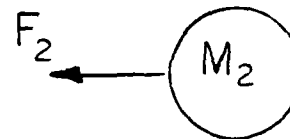
$$x_2 = \frac{w_2^2}{w^3} V_o \sin wt + V_o \left(1 - \frac{w_2^2}{w^2}\right)t + l \quad (A23)$$

and

$$\dot{x}_2 = \frac{w_2^2}{w^2} V_o \cos wt + V_o \left(1 - \frac{w_2^2}{w^2}\right)$$



$$F_1 = K(X_2 - X_1 - L)$$



$$F_2 = -K(X_2 - X_1 - L)$$

Figure A1. Simplified model

## DISTRIBUTION LIST

Commander  
Armament Research, Development and  
Engineering Center  
U.S. Army Armament, Munitions and  
Chemical Command  
ATTN: SMCAR-IMI-I (5)  
SMCAR-AE, B. W. Bushey  
SMCAR-AET, W. Ebihara (2)  
SMCAR-AET-A, R. Kline  
N. Ng  
W. Koenig (10)  
J. Murnane  
J. Thomasovitch  
SMCAR-FSP, R. Reisman  
SMCAR-FSP-I, V. Marchese  
D. Chung  
Picatinny Arsenal, NJ 07806-5000

Commander  
U.S. Army Armament, Munitions and  
Chemical Command  
ATTN: AMSMC-GCL  
Picatinny Arsenal, NJ 07806-5000

Administrator  
Defense Technical Information Center  
ATTN: Accessions Division (12)  
Cameron Station  
Alexandria, VA 22304-6145

Director  
U.S. Army Materiel Systems Analysis Activity  
ATTN: AMXSU-MP  
Aberdeen Proving Ground, MD 21005-5066

Commander  
Chemical Research, Development and  
Engineering Center  
U.S. Army Armament, Munitions and  
Chemical Command  
ATTN: SMCCR-MSI  
Aberdeen Proving Ground, MD 21010-5423

Commander  
Chemical Research, Development and  
Engineering Center  
U.S. Army Armament, Munitions and  
Chemical Command  
ATTN: SMCCR-RSP-A  
Aberdeen Proving Ground, MD 21010-5423

Director  
Ballistic Research Laboratory  
ATTN: AMXBR-OD-ST  
AMXBR-LFD, C. Murphy  
L. MacAllister  
W. Mermegan  
V. Oskay  
Aberdeen Proving Ground, MD 21005-5066

Chief  
Benet Weapons Laboratory, CCAC  
Armament Research, Development and  
Engineering Center  
U.S. Army Armament, Munitions and  
Chemical Command  
ATTN: SMCAR-CCB-TL  
Watervliet, NY 12199-5000

Commander  
U.S. Army Armament, Munitions and  
Chemical Command  
ATTN: SMCAR-ESP-L  
Rock Island, IL 61299-6000

Director  
U.S. Army TRADOC Systems Analysis Activity  
ATTN: ATAA-SL  
White Sands Missile Range, NM 88002

Commander  
Harry Diamond Laboratories  
ATTN: DELHD-TI, Library  
2800 Powder Mill Road  
Adelphi, MD 20783-1197

Director  
Advanced Research Projects Agency  
Department of Defense  
Washington, DC 20301

Chief  
Bureau of Naval Weapons  
Department of the Navy  
ATTN: DIS-33  
Washington, DC 20360

Commander  
Naval Ordnance Systems Command  
ATTN: ORD 0323B1, J. V. Costello  
Washington, DC 20360

Commandant  
Marine Corps Development Center  
ATTN: Firepower Division  
Quantico, VA 22134

Commander  
Marine Corps  
Department of the Navy  
ATTN: A04F  
Washington, DC 20360

Commander  
U.S. Naval Surface Weapons Center  
White Oak Laboratory  
ATTN: Research Library  
White Oak, Silver Spring, MD 20910

Commander  
U.S. Naval Ship Research and  
Development Center  
ATTN: Aerodynamics Laboratory  
Washington, DC 20007

Department of the Army  
Office, Chief of Research Development and  
Acquisition  
ATTN: DAMA-CSS-N  
DAMO-SSN  
Washington, DC 20310

Commander  
U.S. Army Materiel Command  
ATTN: AMCDRD-RS-PE-BAL  
5001 Eisenhower Avenue  
Alexandria, VA 22304

Commander  
U. S. Army Missile Command  
U.S. Army Missile Laboratory  
ATTN: AMSMI-RDK  
Redstone Arsenal, AL 35898-5252

Commander  
U.S. Naval Weapons Center  
ATTN: Code 5557  
Technical Library  
China Lake, CA 93555

Commander  
Air Proving Ground Center (PGTRI)  
ATTN: Technical Library  
Eglin Air Force Base, FL 32542

Commander  
U.S. Naval Surface Weapons Center  
Dahlgren Laboratory  
ATTN: Technical Library  
Dahlgren, VA 22448

Director  
NASA Ames Research Center  
ATTN: Technical Library  
Moffett Field, CA 94035

Director  
U.S. Army Aeronautical Laboratory  
Moffett Field, CA 94035

Headquarters  
Air Force Weapons Laboratory  
ATTN: Technical Library  
Kirtland Air Force Base, NM 87117

Avco Corporation  
Avco Systems Division  
ATTN: T. Kane  
201 Lowell Street  
Wilmington, MA 01887

Aerojet ElectroSystems  
ATTN: D. Pillasch  
1100 West Hollyvale Street  
Azusa, CA 91702

Honeywell, Inc.  
Defense Systems Division  
ATTN: G. Stilley  
10400 Yellow Circle Drive  
Minnetonka, MN 55343